BOSON PEAK IN TRANSITIONALLY ORDERED AND ORIENTATIONALLY DISORDERED PHASES

Marc Bernet Garcia

June 2020

A thesis presented for the degree of
Engineering Physics

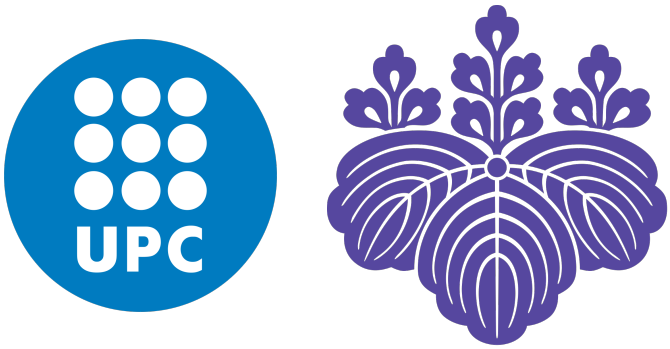

Codirectors: Josep Lluis Tamarit[(a)], Tatsuya Mori[(b)]

[(a)] *Grup de Caracterització de Materials, Departament de Fisica, EEBE and Barcelona Research Center in Multiscale Science and Engineering, Universitat Politècnica de Catalunya, Eduard Maristany, 10-14, 08019 Barcelona, Catalonia, Spain*

[(b)] *Division of Materials Sciences, University of Tsukuba, 1-1-1 Tennodai, Tsukuba, Ibaraki 305-8573, Japan*

Boson Peak in transitionally ordered and orientationally disordered phases

Dielectric study of disordered organic crystals

Marc Bernet Garcia

Abstract

Disordered crystals and glasses have been subject of debate because of its abnormal behavior on their dielectric and thermodynamical properties. In the following work a set of two samples consisting on orientationally disordered but translationally ordered crystals have been studied in order to analyze their excess vibrational modes with respect to the Debye model, also called Boson Peak, at different temperatures. The two materials considered are Pentachloronitrobenzene (PCNB) and 1-Fluoroadamantane (1-FAda) and will be analysed by means of with a THz-Time Domain Spectroscopy system (THz-TDS). They both present glassy anomalies and our results show how a minimal amount of disorder in the translationally ordered lattices gives out the presence of low-energy optic phonons (collective vibrations) that hybridize with the ordinary acoustic phonons, producing an excess of vibrational states that gives rise to the Boson Peak.

Keywords: Boson Peak, THz-TDS, Hybridization.

Acknowledgements

I want to thank firstly the administration and staff at Tsukuba University for providing me the best they could during one of the toughest years anyone has experienced as of yet. Specially I thank Prof. Tatsuya Mori for accepting me in his laboratory and letting me use their resources for the sake of my project, as well as all of my colleagues that taught me through my stay: Kou-kun, Dan-kun, Kim-kun and Nakagawa-kun.

I would then have to thank Prof. Josep Lluis Tamarit for being the main reason why this project could be possible, without his constant help despite the distance and the circumstances, he has proven the most fundamental academic support during my whole research. I am deeply grateful.

Per a vosaltres Sergi, Mama i Papa, moltes gràcies per tot.

Contents

1 Introduction **9**

2 Background **11**
2.1 Vibrational Models 13
2.1.1 Smearing out van Hove singularity 13
2.1.2 Fluctuating elasticity model 13
2.1.3 Soft Potential Model 14
2.1.4 Nonaffine/inversion-symmetry model 14
2.1.5 The fracton model 14
2.1.6 Low-Energy optical phonon hybridization 15

3 Materials **17**
3.1 Pentachloronitrobenzene 17
3.2 1-Fluoroadamantane 21

4 Setup and measurement **24**
4.1 THz-TDS 24
4.1.1 Data Processing 26
4.2 Sample preparation 28

5 Results **31**
5.1 PCNB Results 31
5.2 1-FAda Results 34

6 Discussion **38**
6.1 PCNB discussion 38
6.2 1-FAda discussion 42

7 Conclusions **44**

8 Further work **46**

A Boson Peak frequency as a function of temperature on PCNB **47**

List of Figures

2.1 Exhibit of the glassy properties of Freon-112 and Freon-113 12

2.2 Calculated full frequency distribution of 2-Adamantanone by means of Density Functional Theory following the Perdew, Burke, and Ernzerhof (PBE) approach as implemented in the CASTEP code, using on the fly pseudopotentials. 16

2.3 Calculated dispersion branches along the crystal principal directions of the reciprocal lattice for the set of lower frequency modes. Indices in abscissas correspond to symmetry points of the recpirocal lattice. . 16

3.1 (a) Unit cell of PCNB crystal. The superposed atoms display occupational probability. (b) Different PCNB layers with their respective dipoles, defined by the occupational disorder. 18

3.2 Specific heat data plotted as C_p/T vs T^2 at low temperatures for crystalline PCNB, and its consequent fittings. 18

3.3 (a) Debye-reduced specific heat data C_p/T^3 for the low-temperature crystalline phase of PCNB. The dashed curve indicates the Debye coefficient previously obtained. The upturn of the curve below 1 K is a signature of a quasilinear contribution to the specific heat ascribed to the existence of glassy TLS. Inset: Specific heat data Cp(T) showing the jump corresponding to the glassy temperature. (b) Log-log plot of the thermal conductivity as a function of temperature for PCNB low-dimensional glassy crystal. For comparison, the orientational glasses of ethanol (orange solid circles) and CN-cyclohexane (open circles), and the canonical glass of iso-butanol (green squares), are also shown. (c) Vibrational density of states $g(\omega)$ for the low-temperature crystalline phase of PCNB derived from INS measurements. The dashed red curve corresponds to the Debye approximation valid at the lower frequencies. Inset: Reduced VDOS $[g(\omega)/\omega^2]$ for the data in the main figure. 20

3.4 TR-SHG curves obtained for the phase transition of 1-F-A. Black square, upon cooling (1 K/min); red spot, upon heating (1 K/ min). The signal appears/disappears at 178 K and increases with lowering the temperature down to 100 K. 21

3.5 Crystal structure of 1-FAda. It is clear the centrosymmetry is lost on the mid temperature (b) to low temperature (a) transition. 22

3.6 (a) Debye-reduced specific heat data C_p/T^3 for 1-FAda including 2-Adamantanone and 1-Cyanoadamantane for comparison. We see a clear presence of the Boson Peak around 12K. (b) Vibrational density of states $g(\omega)$ for 1-FAda derived from INS measurements on its low-temperature phase. The red curve corresponds to the Debye approximation valid at the lower frequencies. Inset: Reduced VDOS $[g(\omega)/\omega^2]$ for the data in the main figure. 23

4.1 Asynchronous optical sampling when obtaining THz wave profile. The delay phase is changed throughout and the measured current depicts the wave profile. 24

4.2 Schematic of the functioning of the THz-TDS setup. 25

4.3 (a) Optics system for THz-TDS measurement. (b) Cryostat inserted into the measuring chamber. 28

4.4 Photographs of PCNB before (a) and after (b) being subject of 24h of vacuum. 29

4.5 HDP cast used to contain powder 1-FAda. 30

5.1 THz-TDS measurement of PCNB at room temperature. On the spectra we can clearly see the two higher frequency peaks regarding librations and torsions of the NO_2 group around 3THz. The lower frequency peak at 1THz which is assumed to be a group libration is also seen. 32

5.2 Imaginary part of the complex dielectric permittivity vs temperature for a PCNB heating THz-TDS measurement from 13K up to room temperature at 1THz on a 2.430mm thick sample. The glassy temperature is appreciated as a drastic gradient change around 190K. . . 32

5.3 Heating THz-TDS measurements of 4.922mm thick PCNB sample from 13K to 295K as a function of frequency. We can clearly see the peak around 1THz assumed to be due to librational modes, and the presence of the Boson Peak becomes clear for temperatures down to 270K at around 0.5THz. For heating rates refer to table 4.1. 33

5.4 Real (a) and imaginary (b) parts of the complex permittivity for a 4.922mm thick PCNB sample in heating THz-TDS measurement from 13K to 295K. 34

5.5 (a) THz-TDS measurement at room temperature of 1.072mm thick 1-FAda sample . This measurement was made at atmospheric pressure given the high vapor pressure of 1-FAda. A characteristic peak at 1.35THz is seen in the absorbance spectrum. (b) THz-TDS measurement at room temperature of 1.5mm thick HDP-sealed 1-FAda sample. This measurement was performed in vacuum, and we can see a resemblance to the non-sealed results. In both cases we see no appearance of the Boson Peak. 35

5.6 Heating THz-TDS measurements of 1.5mm thick 1-FAda sample (in HDP cast) from 14K to 295K as a function of frequency. We can see a clear and broad peak around 1THz, the Boson Peak. For heating rates refer to table 4.2. 36

5.7 Imaginary part of the complex dielectric permittivity vs temperature-for a 1-FAda heating THz-TDS measurement from 14K up to room temperature at 1THz on a 1.5mm thick sample (with HDP cast). The different phases as well as phase transitions are denoted in the graph. 37

6.1 (a) Scheme of the Morse potential (blue curve) versus the harmonic potential (green curve). Instead of having a constant $\hbar\omega$ separation between levels, the Morse potential level spacing decreases as the energy approaches the dissociation energy. (b) Direct comparison of THz-TDS results for a measurement from 13K and 295K run. We see the clear shift of the whole spectra assumed to be caused by diffusivity increase and the Morse potential associated with the system. 39

6.2 Comparison of THz-TDS absorbance divided by frequency squared spectrum of a 4.922mm thick PCNB sample at 13K (blue dots) with Raman susceptibility low-ν Raman scattering measurement of 0.8mm thick PCNB sample at room temperature (red line). VDOS divided by ω^2 obtained from INS measurements is included on the figure below for comparison. 41

6.3 (a) THz-TDS measurement at room temperature of 1-FAda. (b) THz-TDS heating measurement of glassy glucose. We can see the resemblance of the spectra at higher temperatures, so we can assume the trend of glucose to be possibly present in 1-FAda as well. 42

A.1 Boson Peak frequency as a function of temperature on a 4.922mm thick PCNB sample. 47

List of Tables

4.1 Temperature steps table of THz-TDS measurement on heating of PCNB. 26
4.2 Temperature steps table of THz-TDS measurement on heating of 1-FAda. 26

Chapter 1

Introduction

A perfect crystal is defined by S R Elliott as that on which the atoms (or groups of atoms or 'motifs') are arranged in a pattern that repeats periodically in three dimensions to an infinite extent. Whilst amorphous materials are defined as those who do not posses this long range order, and are considered to be glasses if these materials exhibit a glass transition, on which the solid amorphous phase exhibits a more or less abrupt change on its derivative thermodynamic properties, from crystal-like to liquid-like. [1]

These disordered structures we call glasses are characterized differently from its ordered counterparts given the differences they present in some of their measureable properties. Some examples could be the specific heat, thermal conductivity or dielectric absorption, which will be the ones we will essentially discuss in this project.

As a follow-up to the previous work from the Grup de Caracterització de Materials (GCM) at Universitat Politècnica de Catalunya (UPC), we try to account for the origin and causes of these features on specific materials. It has been previously shown by the group the existence of anomalous behaviours on halomethane crystals, giving credit of such results to the freezing-in of atomic disorders shown by the compound. To continue the research we will try to measure the properties of "lowly-disordered" materials and try to shed some light into the issue.

The materials studied and measured are two organic crystalline compounds which exhibit a well known low-dimensional disorder. These are Pentachloronitrobenzene (PCNB) and 1-Fluoroadamantane (1-FAda), and we must say that both structures have already been solved recently and studied deeply (see Thomas et al., Tamarit et al., Cole et al.)[2]-[7]. The fact that these two compounds are crystals makes us think that we will see no typical glassy behaviours, but the low amount of disorder in both materials makes them candidates for some anomalies in the thermodynamic properties with some similarities to the well-known reported for canonical glasses.

Both materials were suspected of possessing these so-called glassy anomalies, and so as we could see in previous measurements for PCNB [2] and 1-FAda [8], these suspicions were not unfounded. We can clearly see the emergence of the Boson Peak on PCNB and for 1-FAda. It was shown during the production of this project that the Boson Peak was also present on its specific heat spectra. In order to translate these

results into saying that both of these materials present an excess on the vibrational density of states (VDOS) we must verify such results with their dielectric absorption, in order to ratify them and to determine the origin of the observed phenomena. Consequently, the aim of this project is to measure and characterize the dielectric response of both of these crystals and determine the phenomena that govern these glassy anomalies.

We will further see that these events are in deep relation with the very debated low-energy optical phonons [9][10][11]. These have been observed via density functional theory (DFT) on some ordered structures of orientationally disordered crystals and are clearly the dominant force causing the emergence of an excess on the VDOS. These phonons are believed to be collective modes that because of the very fact of being collective, can hybridize with the acoustic phonons and give rise to the peak.

Chapter 2

Background

In order to understand all of the phenomena and different theories presented regarding the Boson Peak and glassy anomalies we first must understand the foundations of solid state physics and the thought process that has lead to such debate in the scientific community when it comes to this topic.

The vibrational density of states (VDOS) is the integral over the Brillouin zone that goes over all 3N phonon bands, where N is the number of atoms in the cell, thus describing the distribution by energy of the different vibrational modes that are present in our lattice. It provides information about the energy of the different phonons in the material and can be used to identify dominant phonons, compute thermal conductivity of the material, make judgements on how heat transfers across an interface of dissimilar materials, among other things. [12]

The VDOS of solids can be measured experimentally using inelastic scattering techniques, such as X-ray and neutron scattering, where the dynamic structure factor $S(q, \omega)$ is directly measured. Upon summing over all wavevectors q, the VDOS is obtained. These branches define the different optical and acoustic phonons of our material and carry a lot of information when dealing with the Boson Peak and glassy anomalies. In the case of glassy solids, on the lower frequencies we see an agreement with the Debye law (ω^2). The Debye model states that the specific heat is a consequence of the vibrations of the atoms of the lattice of the solid, with a continuous range of frequencies that cuts off at a maximum frequency ω_D, which is characteristic of a particular solid. This happens though from $\omega = 0$ up to a crossover frequency at which phonons no longer propagate ballistically but start to feel the mesoscopic disordered structure which causes phonon scattering. The combination of disorder-induced and anharmonic scattering leads through a Ioffe-Regel crossover into a regime where vibrational modes propagate in a diffusive-like manner (diffusons). In the frequency range below the Ioffe-Regel crossover, where mean-free path is still bigger than the half wavelength, and the notion of phonon dispersion is well defined, we see a ballistic behaviour. [13][14]

At this crossover, the VDOS normalized by ω^2 features a peak which is what we know as the Boson Peak. On the VDOS spectra ($g(\omega)$) we can clearly see the excess when represented like $g(\omega)/\omega^2$, and thus clearly stating the presence of such excess. The VDOS is directly related to the specific heat, and so we can also measure indi-

rectly the density of states via specific heat measurements, giving us an insight on the frequency range where we can find the Boson Peak. The VDOS is related to the specific heat at constant volume C_V in the following way:

$$C_V(T) = k_B \int_0^\infty \left(\frac{\hbar\omega}{2k_BT}\right)^2 sinh\left(\frac{\hbar\omega}{2k_BT}\right)^{-2} g(\omega)d\omega \tag{2.1}$$

We see in both cases that given the ω^2 and the T^3 dependence for the VDOS and C, the excess we are looking for is not seen on the spectra described by $g(\omega)$ and C, but $g(\omega)/\omega^2$ and C/T^3 [15]. For the specific heat, a peak emerges around a specific temperature, which will translate into a certain energy that can give us an insight on the frequency of dielectric absorption where we will locate the Boson Peak.

All of these glassy anomalies are also seen on the thermal conductivity, as previously mentioned [16]. This is a particularly difficult measure to perform and treat, but we can differentiate glass-like behaviour from crystal-like behaviour. The bell-shaped spectra is characteristic of ordered structures like crystals and whenever we have an amorphous material we will see a plateau appearing at a certain temperature range that coincidentally will be the same as the temperature for the Boson Peak on the C_p/T^3 spectra [17]. This coincidence is widely debated in several cases [16][9], and as of now there have been at least one example of some sort of discrepancy between these two temperatures, which we will see further into the project.

All of these characteristic phenomena of glass-like behaviours are seen on figure 2.1, these are the orientationally disordered phases of Freon 112 and Freon 113 [6], which are not canonical glasses but orientationally disordered phases.

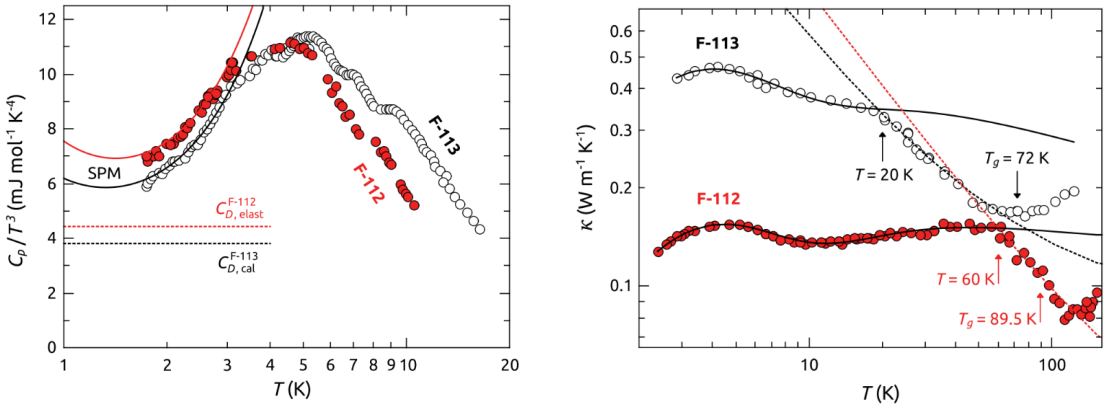

(a) Low-temperature reduced specific heat Cp/T3 for F-112 (full red circles) and F-113 (empty circles), exhibiting the Boson Peak at 4.5 K and 5 K, respectively.

(b) Thermal conductivity as a function of temperature (in log-log scale) for the glassy and plastic crystalline phases of F-113 (empty circles) and F-112 (full red circles).

Figure 2.1: Exhibit of the glassy properties of Freon-112 and Freon-113

Figure 2.1 represents one of the many recorded cases of these glassy features, and since the first reports of the Boson Peak in the mid 50s, it has been observed in polymer glasses, amorphous metal alloys, colloidal glasses, jammed packings, proteins, oxides and of course, orientationally disordered organic crystals. [18][19]

In order to understand the terms of the phenomena that govern these characteristics, we must refer to the different models that are believed to describe the rise of this peak.

2.1 Vibrational Models

2.1.1 Smearing out van Hove singularity

The different ideas with regards to the following are quite disperse. Initially it was believed by various groups that the Boson Peak was a mere excess caused by the presence of Van Hove singularities [20]. Van Hove singularities are those singularities (non-smooth points) present in the VDOS of a crystalline solid, or also addressed as critical points in the Brillouin zone (phonon dispersion relation becomes flat, for example, at the Brillouin boundary). They can be easily identified from the dispersion branches and are believed to appear in all amorphous materials by extension of the Debye model to them. This theory is put into question when analyzing harmonic FCC lattices, where the disorder can be tuned, and we can clearly see two differentiated peaks, with the Boson Peak appearing at lower frequencies, in addition to the van Hove singularity.

2.1.2 Fluctuating elasticity model

In other attempts to explain the phenomena, a great step was made when introducing fluctuating elastic constants in a disordered medium by Schirmacher, Ruocco and co-workers [21][22]. This model is based on the evaluation of the Green's function with a self-consistent Born approximation, assuming that the shear modulus is spatially heterogeneous. It starts by assuming that the shear elastic modulus fluctuates around the material with an average value, considering it follows Gaussian statistics. An elastic Lagrangian is then formulated and the Gaussian disorder assumption leads straightforward to the evaluation of the free energy with quenched disorder and hence to the evaluation of the Green's function.

On its simplest form, the Green function resembles the one of a damped harmonic oscillator:

$$G(z) = \sum_{|k|<k_D} G(k,z) = \sum_{|k|<k_D} \frac{1}{-z^2 + k^2[c^2 - \sum(z)]} \tag{2.2}$$

where $z - \omega + i\epsilon$ ($\epsilon \to 0$), c is the speed of sound, and Σ is the self-energy which contains the effect of multiple scattering of the phonons by the disorder in the elastic modulus. From this expression we can compute the VDOS by using Plemelj identity [23]:

$$g(\omega) = \frac{2\omega}{\pi} Im(G(z)) \tag{2.3}$$

This model unveils the deep connection between vibrational modes that constitute the Boson Peak and the prominence of transverse modes associated with shear elasticity.

2.1.3 Soft Potential Model

The Soft Potential Model (SPM) [24][25][26][27][28] was the first model of its kind in this field trying to explain the density of states in glasses. The model predicts as follows: a set of randomly distributed defects live in a highly anharmonic environment, and experience soft mode-type vibrations which add up onto the Debye phonons thus resulting in the Boson Peak. The assumption of the anharmonic nature of the environment has been shown to not be essential in order for our material to present an excess on its VDOS. It is worth mentioning though that the SPM was the first to predict the existence of quasi-localized modes at lower frequencies than that of the Boson Peak.

The SPM derives from the Standard Tunneling Model, which postulates the ubiquitous existence of small groups of entities, arising as a consequence of some intrinsic disorder. These small groups can tunnel between two configurations of very similar energy, and that's what we call tunneling two-level systems (TLS) [29]. The SPM and the previous STM have been observed to describe phenomena such as TLS (uprise in the C/T^3 spectra when T heads to zero,as we will see further), but fails to describe phenomena observed at milikelvin temperatures and cannot account for all universal glassy behaviours.

2.1.4 Nonaffine/inversion-symmetry model

In a much more specific context, the nonaffine lattice dynamics formalism is based on the idea that atoms in an amorphous material do not occupy centers of inversion symmetry [30][31]. This asymmetry produces a residual force on the atoms, thus producing an additional displacement on the relaxation called the nonaffine displacement. This displacement provides a negative contribution to the internal energy of deformation, and it has been shown that there is a correlation between the Boson Peak height and the degree of inversion-symmetry breaking.

This portrayal closely relates with one of the materials measured, as it has been demonstrated that 1-FAda does posses centrosymmetric and non-centrosymmetric phases [8], as we will discuss further. This model, as we can see, depicts a good unifying framework for both disordered crystals and glasses, which other models do not contemplate.

2.1.5 The fracton model

In 1982 a simple model to describe the VDOS of a fractal was proposed by Alexander and Orbach [32]. Starting from the equation describing the relation between the DOS and the single site Green's function,

$$\rho(\lambda) = -\frac{1}{\pi} Im\langle \tilde{P}_0(-\lambda + i0^+)\rangle \tag{2.4}$$

being $\tilde{P}_0$ the Laplace transform of the function giving out a particle position at time t. If anomalous diffusion is assumed, the mean square displacement becomes the following: $\langle r^2(t)\rangle \sim t^{2/(2+\bar{\delta})}$, being δ the anomalous diffusion index. It is later obtained after a couple of assumptions that $\langle P_0(t)\rangle \sim t^{-\bar{d}/(2+\bar{\delta})}$. When applying

such results to the previously mentioned Green function for the fluctuating elasticity model we end up with the following VDOS:

$$g(\omega) \sim \omega^{2\bar{d}/(2+\bar{\delta})-1} \tag{2.5}$$

This VDOS produces a Ioffe-Regel crossover from propagating phonons o quasilocalized excitations, which are called fractons. These have been widely observed by THz-TDS systems [33][34], and have been formalized via Taraskin's work on THz and IR absorption [35][36][37].

2.1.6 Low-Energy optical phonon hybridization

In the more recent years, and in the case of my group's research project, the Boson Peak has been heavily linked to the disorders present in the lattice, thus, the study of orientationally disordered crystals. The freezing of this molecular disorders seems to give rise to "glassy features", including the Boson Peak. It has been proved all along that the main factors when defining the VDOS on disordered systems are the low-energy optical phonons of the system [9][10][11], and this optical phonons represent collective modes on the lattice and are believed to hybridize with the acoustic phonons. This phenomena could possibly explain the emergence of the Boson Peak and discredit the universal properties of glasses, as their attributed properties are not exclusive to them.

On the most recent measurements performed by GCM, a certain derivative of adamantane was treated, 2-adamantanone [38]. This is an organic orientationally disordered crystal whose ordered phase was found by means of thermal cycles between ca. 100 and 220 K, and thus, DFT calculations were possible for such ordered phase. From the DFT calculations the VDOS and the dispersion branches from the material were visualized. As we can see in figure 2.3, the dispersion branches include at least three very low-energetic optical phonons at around 5meV, and these are believed to be capable of interacting closely with acoustic phonons, given that these optical branches are collective modes. This interaction in some way gives out an excess in the VDOS, the Boson Peak.

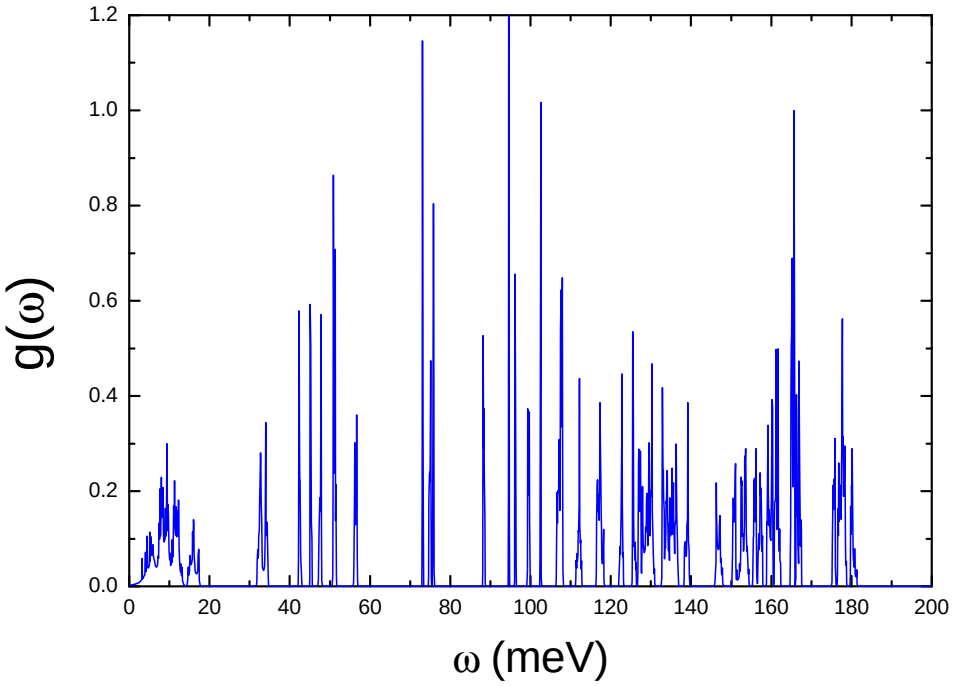

Figure 2.2: Calculated full frequency distribution of 2-Adamantanone by means of Density Functional Theory following the Perdew, Burke, and Ernzerhof (PBE) approach as implemented in the CASTEP code, using on the fly pseudopotentials.

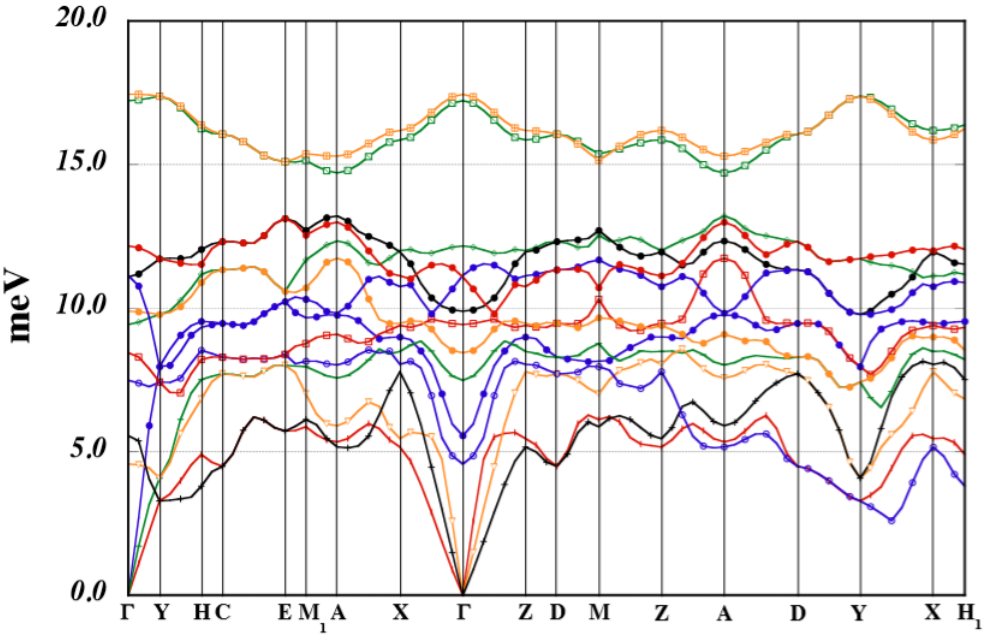

Figure 2.3: Calculated dispersion branches along the crystal principal directions of the reciprocal lattice for the set of lower frequency modes. Indices in abscissas correspond to symmetry points of the recpirocal lattice.

Chapter 3

Materials

The studied materials on this project have both been subject of debate and study and their structures as well as the stability of the different phases have been settled completely. First of all, we must say that both of these compounds are organic crystals that present some kind of built-in disorder on their lattices. They are highly anisotropic and both present glass-like features in their thermodynamic properties.

3.1 Pentachloronitrobenzene

PCNB is a low-dimensional, highly anisotropic organic crystal that displays layered structure of parallel rhombohedral ($R\bar{3}$) planes, on which the molecules are able to rotate around a six-fold-like axis. This disposition ends up with two perpendicular non-zero components on its molecular dipole which we can see on figure 3.1, that possess highly anisotropic dynamical coupling. The larger dipole component has a reorientational motion within the (001) plane of the hexagonal structure, and the small dipole around the c hexagonal axis. Thomas et al.[7] identified the measured source of disorder on PCNB as the reorientational jumps performed by the NO_2 between the 6 possible atomic sites with equal probability ($p_{NO_2} = 1/6$, as seen in figure 3.1, consequently, chlorine atoms are also disordered with equal probability of $p_{Cl} = 5/6$). It was revealed that within the structure, depending on the contacts between hexagonal structures given the disorder induced by the jumps, counter-intuitively, the groups suffered extreme displacements that contribute to the stress induced on the molecule.

Recent studies performed by GCM at UPC show that the glassy features on PCNB measurements are caused by the fact that the reorientational motions may freeze upon cooling or pressurizing [2], resulting in an orientational glass: orientationally disordered phases therefore exhibit a phenomenology that is analogous to that of structural glass formers. It is worth mentioning that the glassy temperature of PCNB was measured to be at around 185K, which will be verified within this project's results.

The measurements performed previously concerning the specific heat, thermal conductivity and density of states at low-temperature are also displayed on figure 3.3 [2]. The description of the specific heat was determined as:

$$C_p = C_{TLS}T + C_D T^3 + C_{sm}T^5 \tag{3.1}$$

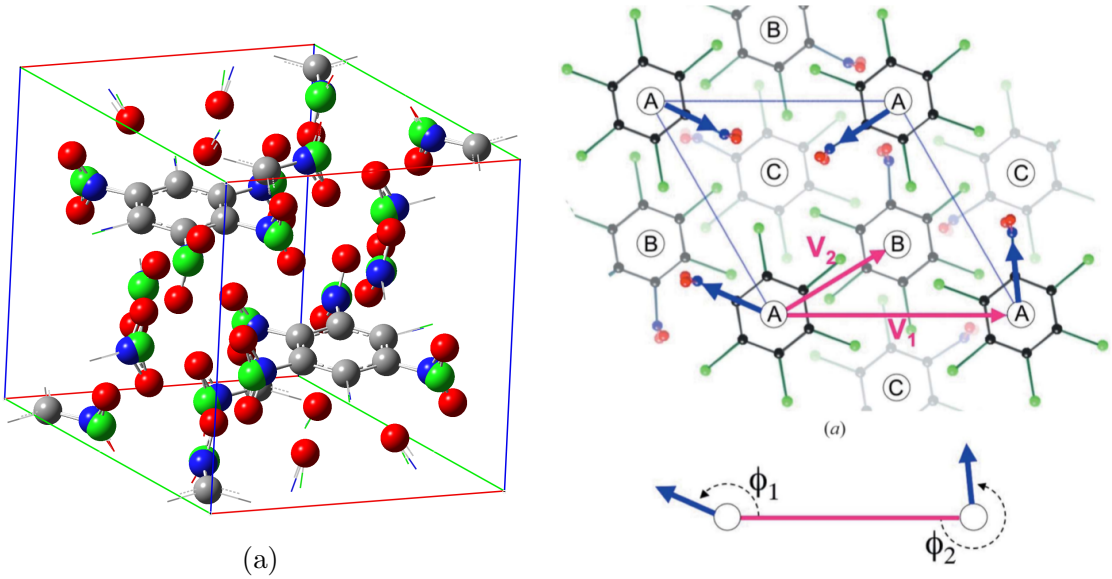

(a) (b)

Figure 3.1: (a) Unit cell of PCNB crystal. The superposed atoms display occupational probability. (b) Different PCNB layers with their respective dipoles, defined by the occupational disorder.

We can see the presence of the aforementioned tunnelling two-level systems at very low temperatures, and the presence of the Boson Peak at around 4.8K. The specific heat was adjusted via C_p/T vs. T^2 spectra, and the fitting left no questions about the different contributions on the specific heat. If we take a look at figure 3.2, we can see that the fitting taking into account the SPM gives out a much better performance, and to consider the fact that the spectra starts at a nonzero value, we must include a TLS term.

This result not only describes the specific heat of the material but shows the deviation from the original Debye model in a pretty graphic way.

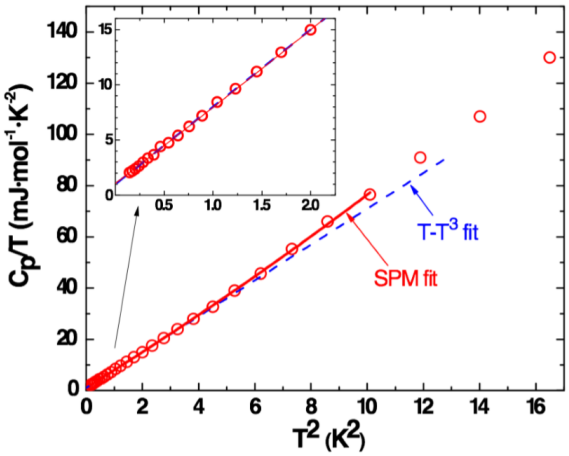

Figure 3.2: Specific heat data plotted as C_p/T vs T^2 at low temperatures for crystalline PCNB, and its consequent fittings.

In terms of the thermal conductivity, it was firstly believed for PCNB to behave abnormally, as the usual plateau associated with the Boson Peak appeared at significantly higher temperatures than 4.8K (appearance at around 40K). But this discrepancy was not given more attention as the measure of the thermal conductivity was started at 5K, thus preventing it from being capable of capturing the plateau in that given range.

The presence of the Boson Peak at 4.8K on the specific heat measurement gives out enough information to determine that the expected Boson Peak position on the dielectric absorption spectra is at about 0.5THz. This suspicion is emphasized by the Inelastic Neutron Scattering measurements of the VDOS, where we can see a peak tendency on the $g(\omega)/\omega^2$ spectrum around $2meV$, but the lack of information of lower energies leaves an interrogant on the matter. We must confirm such suspicions, and determine the exact position of the peak as well as its intensity.

The PCNB sample used in this project has been provided by Sigma-Aldrich (P2205) and has a purity of $\geq 94\%$. The purity stated is enough for the measures to be successful.

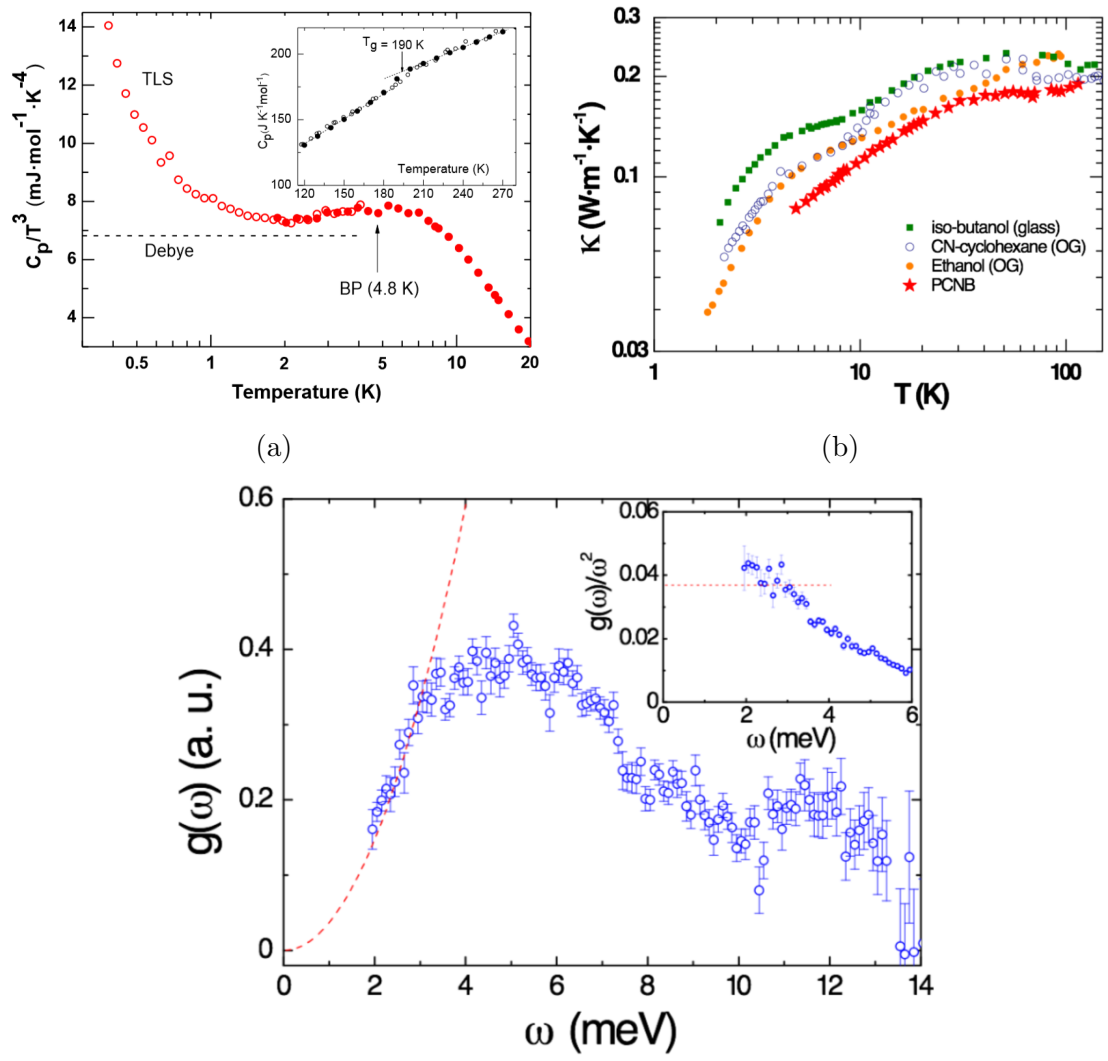

Figure 3.3: (a) Debye-reduced specific heat data C_p/T^3 for the low-temperature crystalline phase of PCNB. The dashed curve indicates the Debye coefficient previously obtained. The upturn of the curve below 1 K is a signature of a quasilinear contribution to the specific heat ascribed to the existence of glassy TLS. Inset: Specific heat data Cp(T) showing the jump corresponding to the glassy temperature. (b) Log-log plot of the thermal conductivity as a function of temperature for PCNB low-dimensional glassy crystal. For comparison, the orientational glasses of ethanol (orange solid circles) and CN-cyclohexane (open circles), and the canonical glass of iso-butanol (green squares), are also shown. (c) Vibrational density of states $g(\omega)$ for the low-temperature crystalline phase of PCNB derived from INS measurements. The dashed red curve corresponds to the Debye approximation valid at the lower frequencies. Inset: Reduced VDOS $[g(\omega)/\omega^2]$ for the data in the main figure.

3.2 1-Fluoroadamantane

1-FAda is an adamantane-derived organic crystal of low-dimensional disorder, on which some glassy anomalies have been observed (as well as in some other adamantane derivatives).

In terms of the structure, 1-FAda presents three different phases. The higher temperature phase, stable from 231 K up to the melting point (525 K), is an orientationally disordered (plastic phase) centrosymmetric cubic $Fm3\bar{m}(225)$, $Z = 4$, in which the Fluorine atoms are disordered (they can occupy 8 positions with equal fractional occupancies of $p_F = 1/8$). On the lower temperatures, from 178K and below, 1-FAda presents an orientationally disordered non-centrosymmetric tetragonal $P\bar{4}21c(114)$, $Z = 2$.

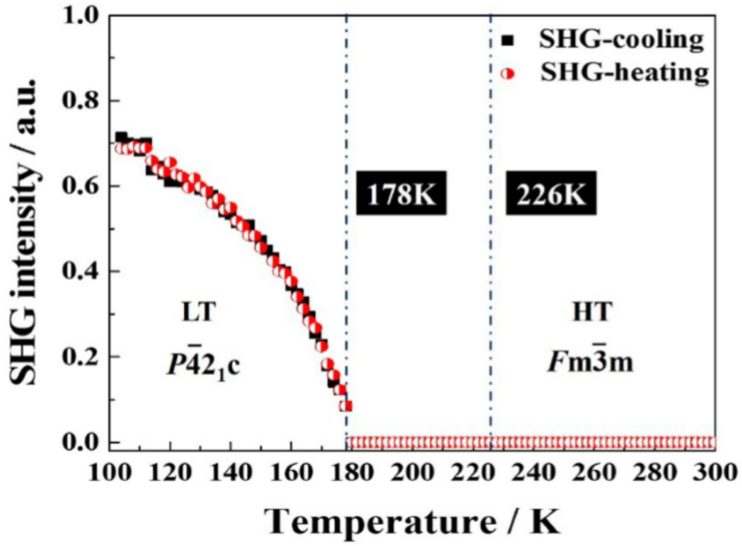

Figure 3.4: TR-SHG curves obtained for the phase transition of 1-F-A. Black square, upon cooling (1 K/min); red spot, upon heating (1 K/ min). The signal appears/disappears at 178 K and increases with lowering the temperature down to 100 K.

On the temperatures between $178K < T < 231K$, an intermediate phase was recently discovered by GCM via Second-Harmonic-Generation (SHG) [8]. The requisite to obtain output signal on SHG measurements is for the measured material to be non-centrosymmetric. A clear margin between the high temperature and low temperature phases did not fit with the previous assumptions (see figure 3.4), as it was believed to be a temperature range on which 1-FAda was on its low temperature phase, and thus, non-centrosymmetric (see in figure 3.5). It was then characterized as a intermediate temperature phase, its structure being an orientationally disordered centrosymmetric tetragonal P42/nmc (137), Z = 2, in which the F atoms can occupy only 4 equivalent sites (fractional occupancy of $p_F = 1/4$). The low-T to intermediate-T phase transition was also identified, and although disorder in the low-temperature phase is quite similar to the intermediate phase, a second order phase transition appears from the intermediate phase to the Low T phase, in such

a way that some symmetry planes disappear and the symmetry of the lattice is reduced (to a non-centrosymmetric structure).

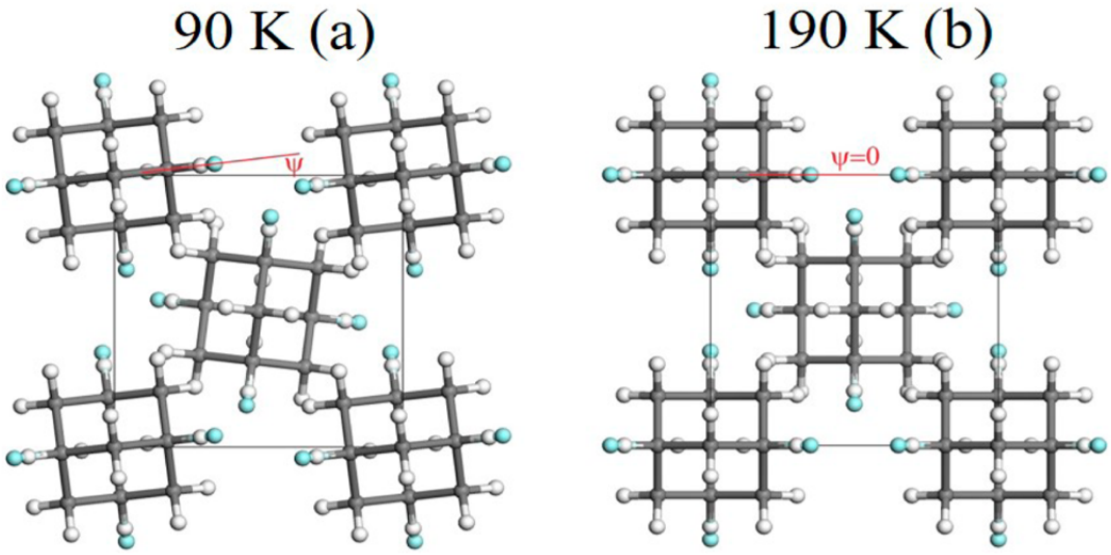

Figure 3.5: Crystal structure of 1-FAda. It is clear the centrosymmetry is lost on the mid temperature (b) to low temperature (a) transition.

As for previous specific heat measurements, we can see in figure 3.6 that there is an apparent Boson Peak at around 11K. As for thermal conductivity, results are still a bit sensitive (thus not included), but there is enough evidence to support the appearance of a plateau at some temperature around 25K, so the glassy behaviour of the material is pretty clear, though it is this project's objective to clarify its features and just as in PCNB, determine the exact position of the peak as well as its intensity.

The 1-FAda sample used in this project has been provided by Tokyo Chemical Industry (F0511) and has a purity of $> 98\%$. The purity stated is enough for the measurements to be successful.

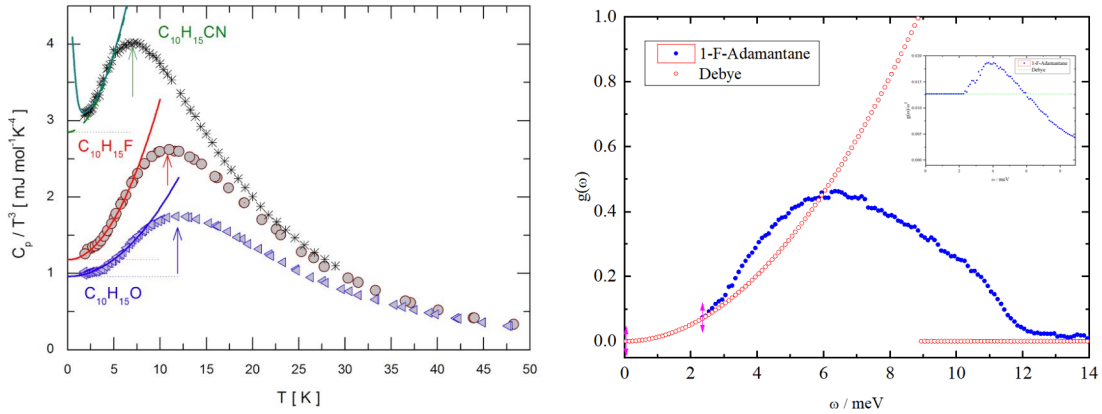

(a) (b)

Figure 3.6: (a) Debye-reduced specific heat data C_p/T^3 for 1-FAda including 2-Adamantanone and 1-Cyanoadamantane for comparison. We see a clear presence of the Boson Peak around 12K. (b) Vibrational density of states $g(\omega)$ for 1-FAda derived from INS measurements on its low-temperature phase. The red curve corresponds to the Debye approximation valid at the lower frequencies. Inset: Reduced VDOS $[g(\omega)/\omega^2]$ for the data in the main figure.

Chapter 4

Setup and measurement

On this current project a very specific setup was used in order to measure both materials. The dielectric spectra was obtained via Terahertz Time-Domain Spectroscopy in the Mori Laboratory at Tsukuba University.

4.1 THz-TDS

THz-TDS has been a scarcely used technology when measuring dielectric properties of materials, either because its novelty or its time-consuming and sensible measuring. Nevertheless, it constitutes a perfect setup when trying to measure the Boson Peak on amorphous materials, given its output range.

The basic idea behind this piece of equipment is the asynchronous optical sampling technology. A laser emitter sends a beam which is beamsplit in two before entering into the main chamber where our sample is placed. One of the beams hits a power-source-connected semiconductor at a certain intensity and frequency which by photoemission will give out an emitted electric field consisting of a THz wave. This THz wave will pass through our sample, thus changing its profile, and will hit a second semiconductor when exiting the chamber. This second semiconductor is also being irradiated by the other output beam from the beamsplitter, right after it has gone through a phase change on the phase-change stage. By the same principles of photoemission ($E \propto \frac{dJ}{dt}$, E being electric field and J being current), if we conduct a current measurement we will see as an output the difference of the emitted wave versus the transmitted wave. As we can control the phase-change stage, a sampling over different phase changes is done, thus giving out the profile of the transmitted electric field, from which dielectric properties are extracted.

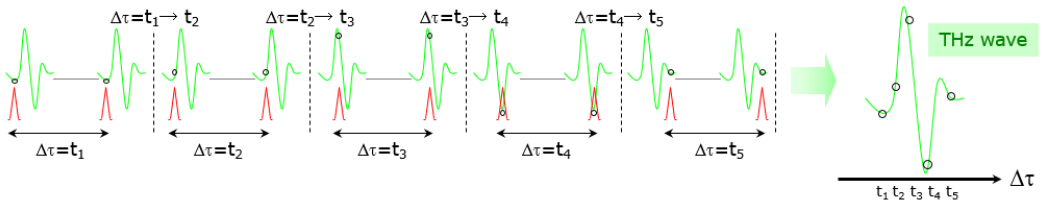

Figure 4.1: Asynchronous optical sampling when obtaining THz wave profile. The delay phase is changed throughout and the measured current depicts the wave profile.

In our project a THz-TDS (RT-10000, Tochigi Nikon Co.) and a liquid-helium flow cryostat system (Helitran LT-3B, Advanced Research Systems) were used with the standard transmission configuration for temperature-dependent measurements in the frequency range of 0.25–2.25 THz from 13 to 295 K. Low-temperature grown GaAs photoconductive antennae were used as emitters and detectors of the THz wave. The THz wave propagation path was enclosed in a dry air chamber within which dry air flows. Cherenkov radiation from a lithium niobate single crystal was used as the light source of the THz wave, covering a frequency band of around 0.5–7.0 THz. Asynchronous optical sampling technology was used for the detection. The THz wave propagation path was purged with dry air. [39][40][36]

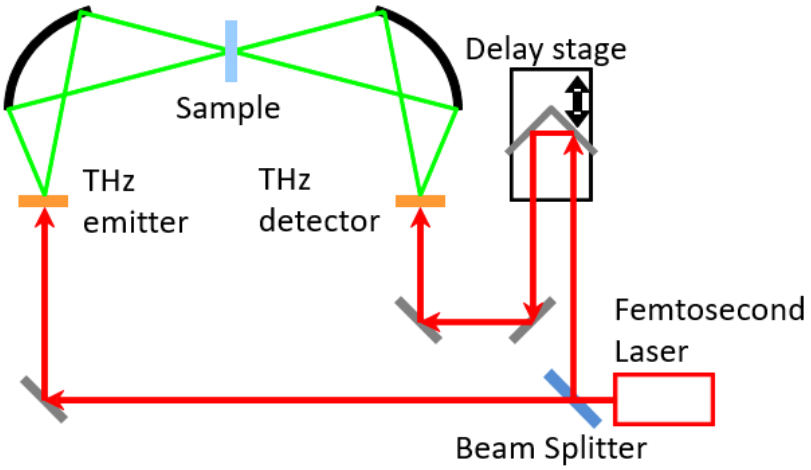

Figure 4.2: Schematic of the functioning of the THz-TDS setup.

For this particular setup, the solid state laser was beamsplit several times before entering the measurement chamber in order for it not to burn down the sample (output power 10meV), as it is organic. Additionally, in order to reduce diffraction when electric waves are photoemitted from the semiconductors, a silicon bead is placed in the opening.

The THz-TDS measurements have been performed with 8192 sampling points for PCNB and 4096 sampling points for 1-FAda. The electric field ($E(t)$) measurement is performed from 0ps to 55ps on PCNB and 0ps to 28ps on 1-FAda. On both materials the resulting $E(t)$ are averaged over 30 different measurement runs for the sample and cell, and 15 different measurement runs for the background.

As for the THz-TDS measurements on heating, the heating rate was 3K/min and the temperatures range from 13K to 295K with the following temperature steps (excluding first and last temperatures, 13K and 295K respectively):

PCNB Temp.	Temp. step
20K-110K	10K
110K-230K	5K
230K-270K	10K
270K-290K	5K

Table 4.1: Temperature steps table of THz-TDS measurement on heating of PCNB.

1-FAda Temp.	Temp. step
20K-170K	10K
170K-190K	5K
190K-220K	10K
220K-240K	5K
240K-290K	10K

Table 4.2: Temperature steps table of THz-TDS measurement on heating of 1-FAda.

4.1.1 Data Processing

The output displayed by the THz-TDS is the electric field measured from the sample and the background runs. When obtaining the transmission spectrum of a sample by transmission type THz-TDS, first the time waveform (reference wave) $E_{ref}(t)$ without the sample is inserted and the time waveform (sample wave) $E_{sam}(t)$ (sample wave of the terahertz pulse wave transmitted through the sample) is measured. Next, these are subjected to fast Fourier transform to obtain the power spectra for each frequency (ω) of the reference wave and the sample wave.

$$E_{ref}(t) \rightarrow E_{ref}(\omega) = E_{ref}(\omega)exp(i\theta_{ref}) \tag{4.1}$$

$$E_{sam}(t) \rightarrow E_{sam}(\omega) = E_{sam}(\omega)exp(i\theta_{sam}) \tag{4.2}$$

From the amplitude ($E_i(\omega)$) and phase ($exp(i\theta_i)$) information obtained by the measurement, the complex amplitude transmission coefficient of the sample is obtained by the following formula:

$$\tilde{t}(\omega) = \frac{E_{sam}(\omega)}{E_{ref}(\omega)} = \left(\frac{E_{sam}(\omega)}{E_{ref}(\omega)}\right) expi(\theta_{sam}(\omega) - \theta_{ref}(\omega)) \tag{4.3}$$

On the other hand, when the THz pulse wave is transmitted through the parallel plate sample having the thickness d, the theoretical value of the complex amplitude transmission coefficient ($\tilde{t}(\omega)$) can be expressed as follows:

$$\tilde{t}(\omega) = \frac{E_{sam}(\omega)}{E_{ref}(\omega)} = \frac{4\tilde{n}}{(\tilde{n}+1)^2} exp\left(i\frac{(\tilde{n}-1)}{c}\omega d\right) \tag{4.4}$$

The complex index of refraction ($\tilde{n}$) is determined so that the theoretical complex transmission coefficient is calculated from equation 4.4. The complex refractive index and the complex permittivity ($\tilde{\epsilon}(\nu)$) then hold this final relation:

$$\tilde{n}^2 = (n + i\kappa)^2 = \tilde{\epsilon}(\nu) = \epsilon' + i\epsilon'' \tag{4.5}$$

being n and κ the real and imaginary values of the complex refractive index, and ϵ' and ϵ'' the real and imaginary parts of the complex permittivity (which we will call dielectric coefficients). Once we know how to express the dielectric coefficient values, then we can proceed to obtain the absorption α. This is easily calculable by just following the simple relation:

$$\alpha(\nu) = \frac{2\pi\nu \cdot \epsilon''}{c \cdot n(\nu)} \tag{4.6}$$

Where ν is the frequency, ϵ'' is the imaginary dielectric coefficient, c is the speed of light and $n(\nu)$ is the index of refraction. From that point, in order to obtain a more clear picture of the Boson Peak, as previously stated, we perform a simple division on α by ν^2. The fact that we analyze α and not $g(\nu)$ is because it is essentially the same. In order to understand how the Boson Peak appears in the THz spectra, we must consider the following relation derived from the linear response theory for disordered materials [41][59]:

$$\alpha(\nu) = C_{IR}(\nu) \cdot g(\nu) \tag{4.7}$$

Being $C_{IR}(\nu)$ the coupling coefficient for IR radiation. Thus, the appearance of the Boson Peak in α/ν^2 is obvious [42]. In fact, we could also compare ϵ'' with α given that:

$$\epsilon'' \approx \alpha k$$

$$\nu k \propto \alpha$$

$$\frac{\epsilon''}{\nu} \propto \frac{k}{\nu} \propto \frac{\alpha}{\nu^2} \tag{4.8}$$

With ϵ'' being the imaginary dielectric coefficient, α being the absorption, k being the wavenumber and ν being the frequency. So from both the dielectric coefficient and the absorbance spectra we can obtain the contribution of the vibrational modes to the density of states as well as the different relaxations appearing on the system. With the given variables we can easily characterize the dielectric behaviour of our measured material on the THz frequency range, as we will see in the results section.

It must be said that given the sensibility of the machinery to changes in thickness of the sample, a uniform and extended measurement throughout all frequencies measurable is impossible, and thus, in some cases we have performed merges of the results to give out the full spectra. In other cases, as it will be displayed, some spectra suffer from heavy noise issues when hitting certain low or high frequencies. These ranges depend on the intrinsic values of the material, as the forementioned thickness of the sample.

4.2 Sample preparation

In this section we will specify on more clearer notes how the samples were treated and modified, and how the material were processed in order for it to be able to yield out good spectra in a THz-TDS measurement.

Both PCNB and 1-FAda samples were fabricated so that they could fit the cylindrical sample holders of the THz-TDS system and so that they could be attached to the cryostat that places the sample in the measurement chamber. Photographs of the system are seen in figure 4.3. PCNB's sample holders are 1cm in diameter and ranged from 1.5mm to 5mm deep, thus having enough options when measuring differently thick samples. For 1-FAda, its sample holders were 2cm in diameter, and given its size, the samples were glued onto the sample holders with vacuum grease, which can still perform on low temperatures.

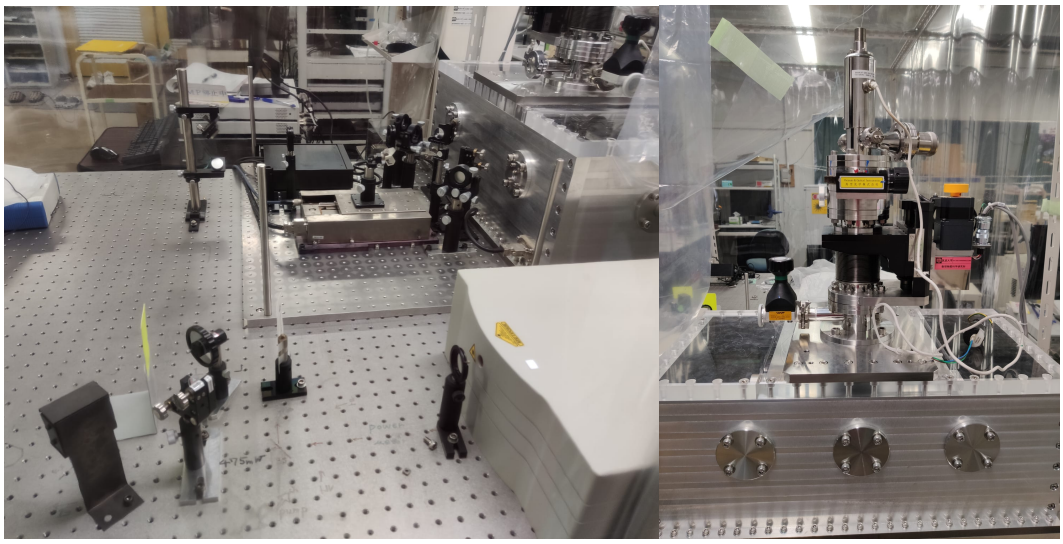

(a) (b)

Figure 4.3: (a) Optics system for THz-TDS measurement. (b) Cryostat inserted into the measuring chamber.

As previously mentioned, it was unclear on the first measurements of PCNB whether the sample was giving out bad data because of the impurities of the material or simply because of bad methodology. It was later determined that the inconsistency came from the broad distribution of far too large grain sizes, which favoured phonon dispersion when these borders were hit. In order to remedy that, PCNB was carefully grounded whilst preventing it from interacting with the media, as it can react with water or reduce. The samples were prepared on a sample press at a maximum pressure of 2MPa and with posterior cooling so that the sample didn't embed onto the cast.

It was also necessary to determine the sample thickness, which consists the most determinant variable on THz-TDS measurements, as it defines the frequency range on which the user will obtain valid spectra. In general, the thicker the sample the

lower will your starting valid spectra frequency be. So, in order to obtain complete visibility from 0.25THz up until 5THz, at least three measurements were required from thicker to thinner samples. It was eventually determined after several measurements that the perfect thickness to determine the Boson Peak on PCNB whilst not losing too much resolution is 5mm, and in order to show the higher frequency region, at least a 0.8mm thick sample is needed.

It must be noted that in the case of PCNB, the constant vacuum by the turbomolecular pump did produce some mass loss for thinner samples, but not enough to interfere with the data. The loss of mass in samples is denoted by a darkening on the sample (probably due to moisture loss) as seen in figure 4.4, which was at first believed to be some reaction but was later discarded by Raman Spectroscopy of the samples as well as IR-Spectroscopy. The option of the darkness due to burning was also discarded, as the laser used does not have enough power to produce such reactions.

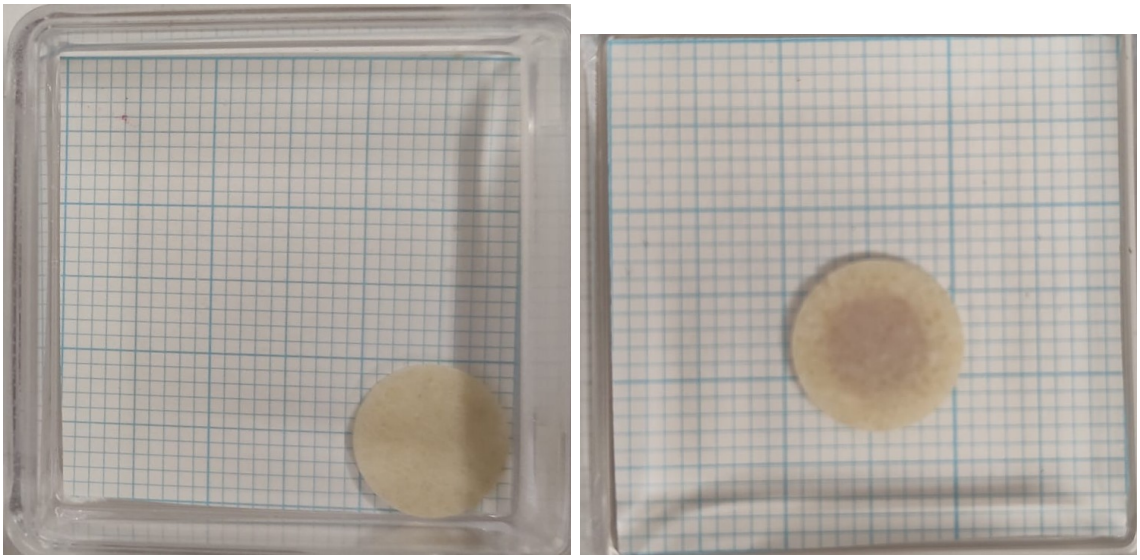

(a) (b)

Figure 4.4: Photographs of PCNB before (a) and after (b) being subject of 24h of vacuum.

As for 1-FAda, the problems manifested themselves notoriously when trying to measure samples on vacuum. The sample preparation process was applied similarly to PCNB, and the atmospheric pressure measurements did not present any problems. When under vacuum conditions, the high vapor pressure from 1-FAda made the sample evaporate and thus interfering with the measurements. The solutions available were nitrogen purging during cooling, or simply fabricating a cast to prevent evaporation of the sample, which was the method that yielded out the best results. A High Density Polyethylene (HDP) cast permitted the measurement of powder samples in vacuum, but required a much tougher data processing, thus gaining lots of noise. Nevertheless, the measurements were good enough to observe the absorbance profile. The cast can be seen in figure 4.5.

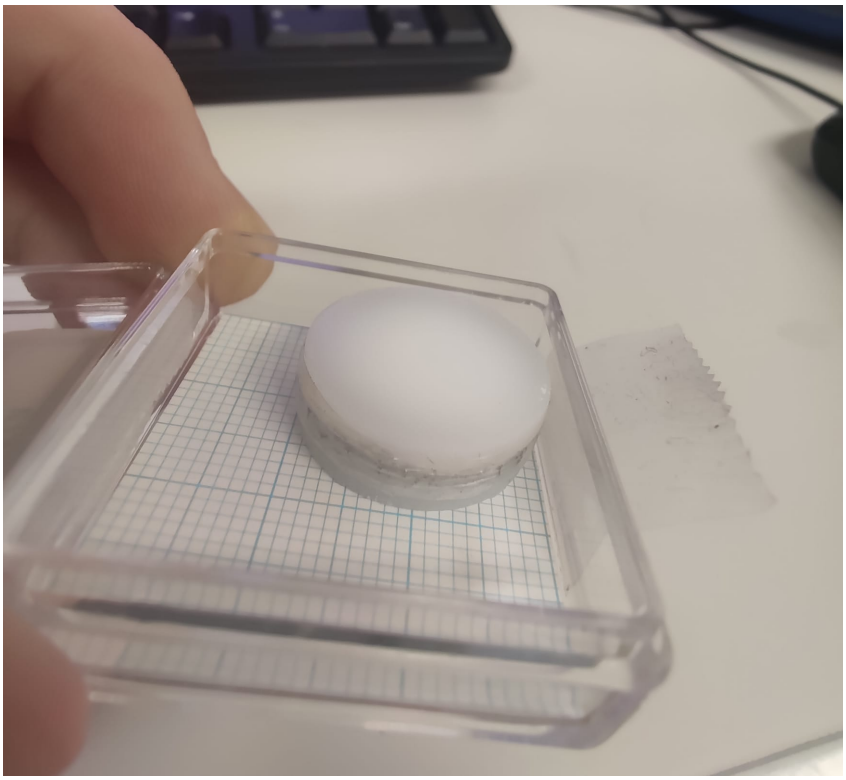

Figure 4.5: HDP cast used to contain powder 1-FAda.

Chapter 5

Results

In the following pages we will discuss the results obtained for each material and try to link those results with the previous information on both.

In the case of THz-TDS measurements, as we have discussed previously, we can obtain the absorbance spectra of both materials for a large range of frequencies as well as a function of temperature. On the THz-TDS setup, measurements from room temperature down to 13K were obtained for both PCNB and 1-FAda materials.

5.1 PCNB Results

For PCNB, it was firstly noticeable that the results were not giving out good spectra because of the grain size of the PCNB crystals, as their large size made scattering and noise effects increase given that the phonon dispersion is strong when hitting grain borders. In order to avoid that problem, PCNB had to be grounded to obtain smoother results.

Measurements of a 4.922mm thick sample and a 1.336mm thick sample at room temperature were merged to obtain the whole spectra as well defined as possible. The end result is presented in figure 5.1. As we can see the absorption spectrum presents three well defined peaks at first glance, located at around 1THz, 2.7THz and 3.3THz. The profile of the spectrum matches previous measurements of PCNB on the far-infrared, thus giving a sense of validity to the results [5]. In this previous study the higher frequency peaks are linked to intramolecular modes caused by the NO_2 group torsions, whereas the lower frequency peak is assumed to be some sort of libration or torsional motion of the whole molecule about their pseudo-6-fold axis. These findings will be put into perspective with our own findings and we will be able to verify such assumptions. It is also worth reporting that the previous data on PCNB's glass temperature [2] matches the results obtained, as seen in figure 5.2, where we plot the imaginary part of the dielectric permittivity as a function of temperature at constant frequency (1THz).

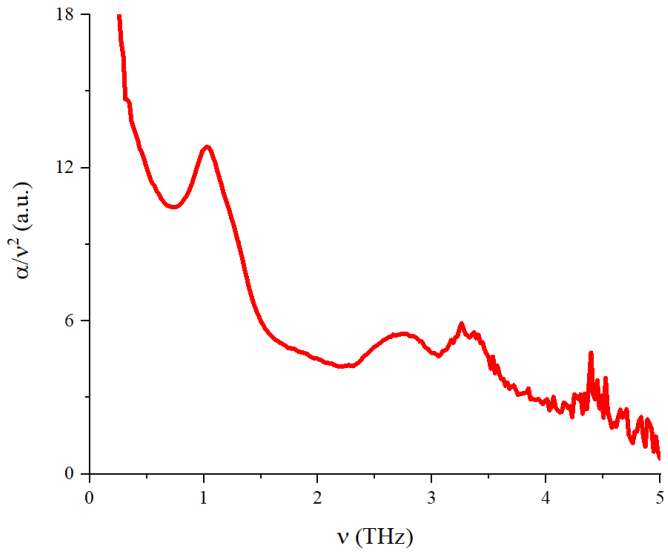

Figure 5.1: THz-TDS measurement of PCNB at room temperature. On the spectra we can clearly see the two higher frequency peaks regarding librations and torsions of the NO_2 group around 3THz. The lower frequency peak at 1THz which is assumed to be a group libration is also seen.

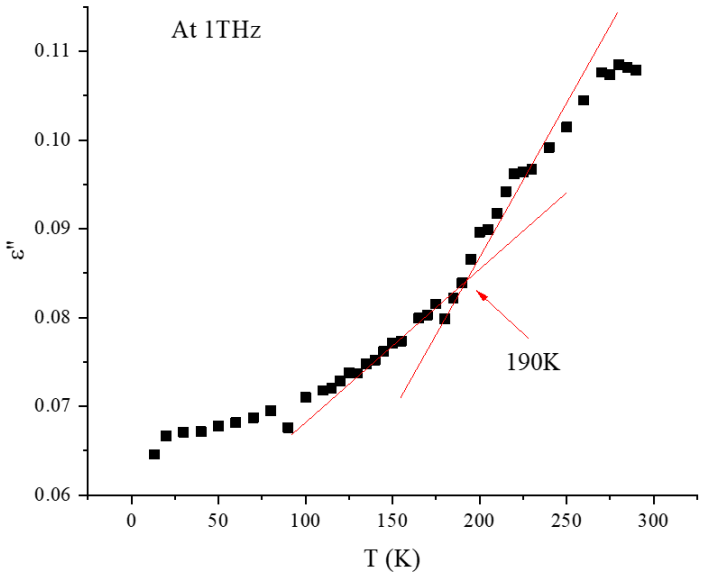

Figure 5.2: Imaginary part of the complex dielectric permittivity vs temperature for a PCNB heating THz-TDS measurement from 13K up to room temperature at 1THz on a 2.430mm thick sample. The glassy temperature is appreciated as a drastic gradient change around 190K.

In this project we are not interested in the higher frequency modes, as they do not interact with the Boson Peak, but the 1THz peak does spark some interest as its nature is still not clear and could provide interesting information to the discussion. It must be said that at such temperatures the Boson Peak could not be seen on the spectra, even though its expected position was at about 0.5THz ($\sim 2meV$).

Now, for a more specific visualization of the Boson Peak, a measurement on heating the 4.922mm thick sample was performed, ranging from 13K to 295K with decreasing heating rates around the PCNB glassy temperature (around 185-190K). The results are shown in figure 5.3 and 5.4.

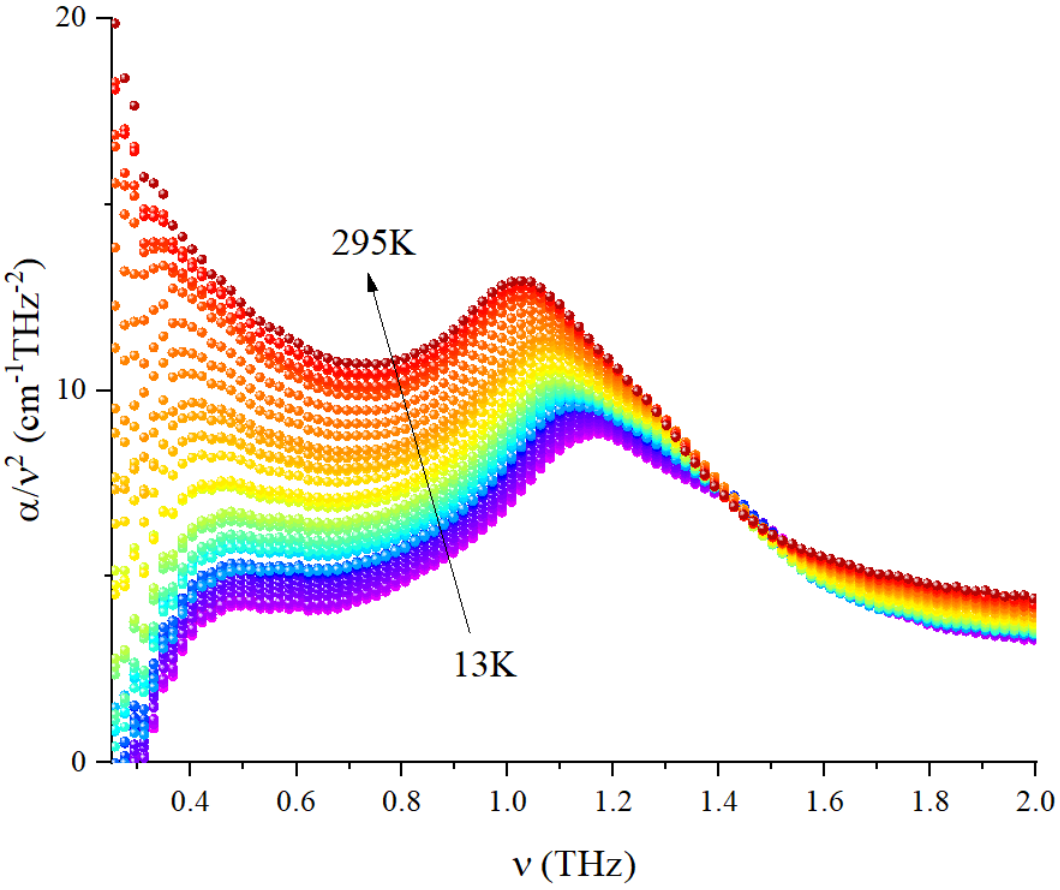

Figure 5.3: Heating THz-TDS measurements of 4.922mm thick PCNB sample from 13K to 295K as a function of frequency. We can clearly see the peak around 1THz assumed to be due to librational modes, and the presence of the Boson Peak becomes clear for temperatures down to 270K at around 0.5THz. For heating rates refer to table 4.1.

From these data we can perfectly locate the Boson Peak at 0.45THz (∼5THz) in agreement with previous inelastic neutron scattering measurements (2meV, 0.48THz), and its presence can be detected at temperatures around 270K and below. The Boson Peak at room temperature is non detectable because of the activation of the α-relaxation at around that frequency, which overwhelms the presence of the Boson Peak. We can also appreciate the presence of the Boson Peak in the dielectric coefficients ϵ' and ϵ'', just like we can see in figure 5.4

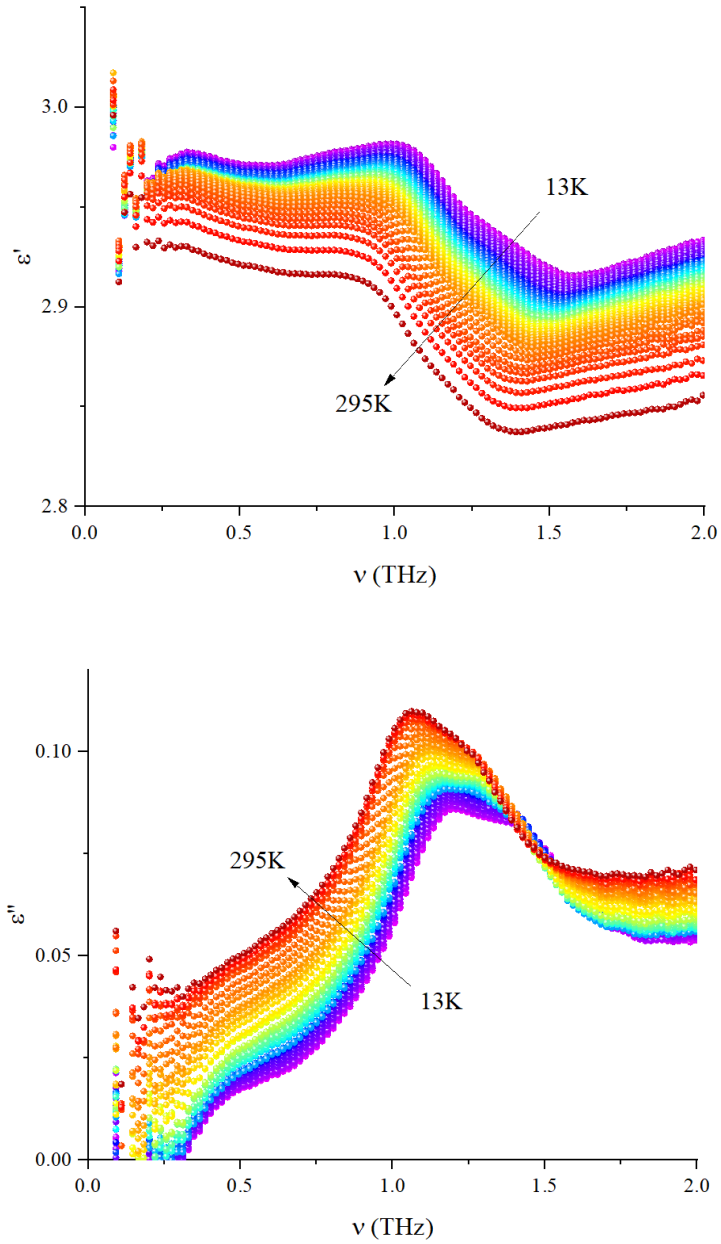

Figure 5.4: Real (a) and imaginary (b) parts of the complex permittivity for a 4.922mm thick PCNB sample in heating THz-TDS measurement from 13K to 295K.

5.2 1-FAda Results

The measure of 1-FAda presented a couple of obstacles that have been mentioned previously as they introduce some noise to the overall measurements.

1-FAda's vapour pressure has a high value, and when in continuous vacuum produced by a turbomolecular pump during a considerable period of time, the sample will end up losing mass and eventually sublimating completely. This problem had

to be solved either by nitrogen purging or by sealing off the sample with High Density Polyethylene (HDP). It is known and has been observed in previous results by Mori's Laboratory that HDP does not contribute by no means to the spectra at the measured frequencies, despite it increasing the noise and scattering of the output signal.

For quick room temperature measurements though, no sealing was necessary, and we could obtain the spectrum presented in figure 5.5. We can see that the Boson Peak is smeared out at room temperature, although we would match the absorbance results with previous measurements on 1-FAda, thus giving once again validity to the measurement [43]. This result is not surprising, as at this range of temperatures, just as the case with PCNB, we can have a strong influence of the α-relaxation that boost the spectra in a way that masks the presence of the Boson Peak. Another option to describe this could be that in this specific phase of 1-FAda there is no Boson Peak, which would be surprising, as all of the 1-FAda phases present orientational disorder. As for the sealed measurements, we could see a great increase of the noise captured on our results, but via analysis, processing and thorough cleaning of the data we could obtain a somewhat clear view of 1-FAda's absorption at room temperature. The results are displayed on figure 5.5.

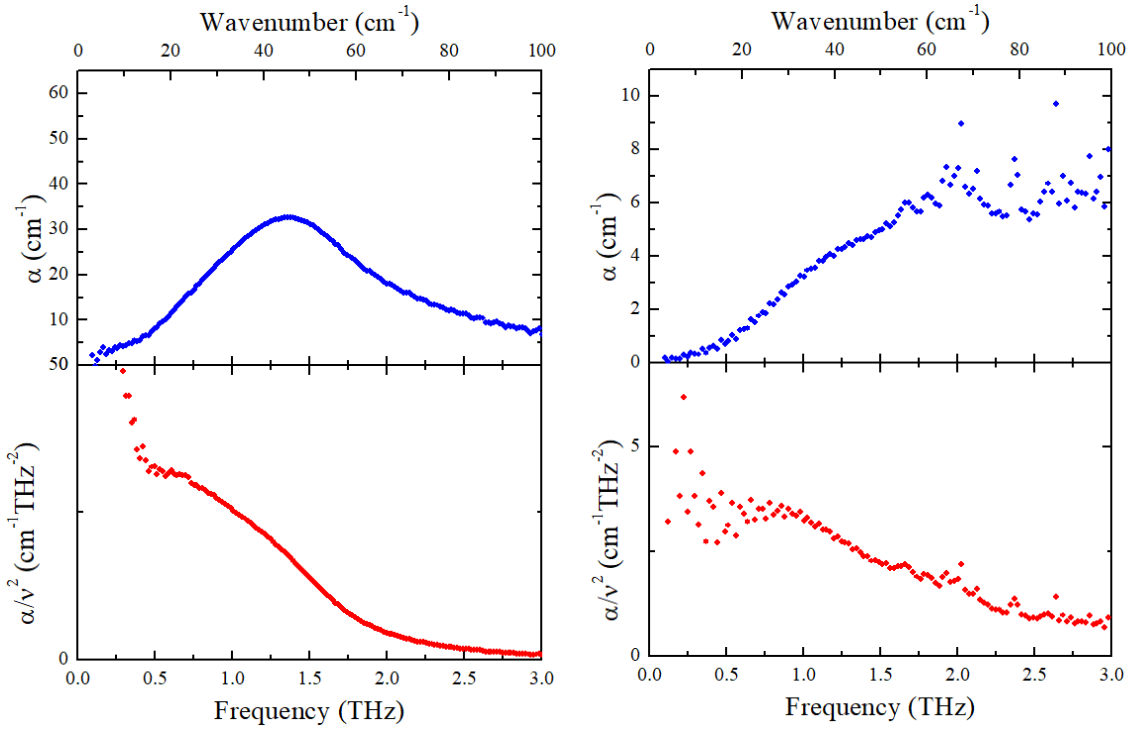

(a) (b)

Figure 5.5: (a) THz-TDS measurement at room temperature of 1.072mm thick 1-FAda sample . This measurement was made at atmospheric pressure given the high vapor pressure of 1-FAda. A characteristic peak at 1.35THz is seen in the absorbance spectrum. (b) THz-TDS measurement at room temperature of 1.5mm thick HDP-sealed 1-FAda sample. This measurement was performed in vacuum, and we can see a resemblance to the non-sealed results. In both cases we see no appearance of the Boson Peak.

After data processing to eliminate noise as much as possible, our heating measurement of 1-FAda on temperature from 14K to 295K gave out the results seen on figure 5.6. Despite the clear noise of the measurement, we can appreciate a clear presence of a broad peak at 1THz. This is believed to be, given the previous measurements performed, the Boson Peak. Given the nature of the heating measurement, we have no presence of the α-relaxation we noticed on the room temperature measurements, that prevented the Boson Peak from appearing. In order to verify the validity of the

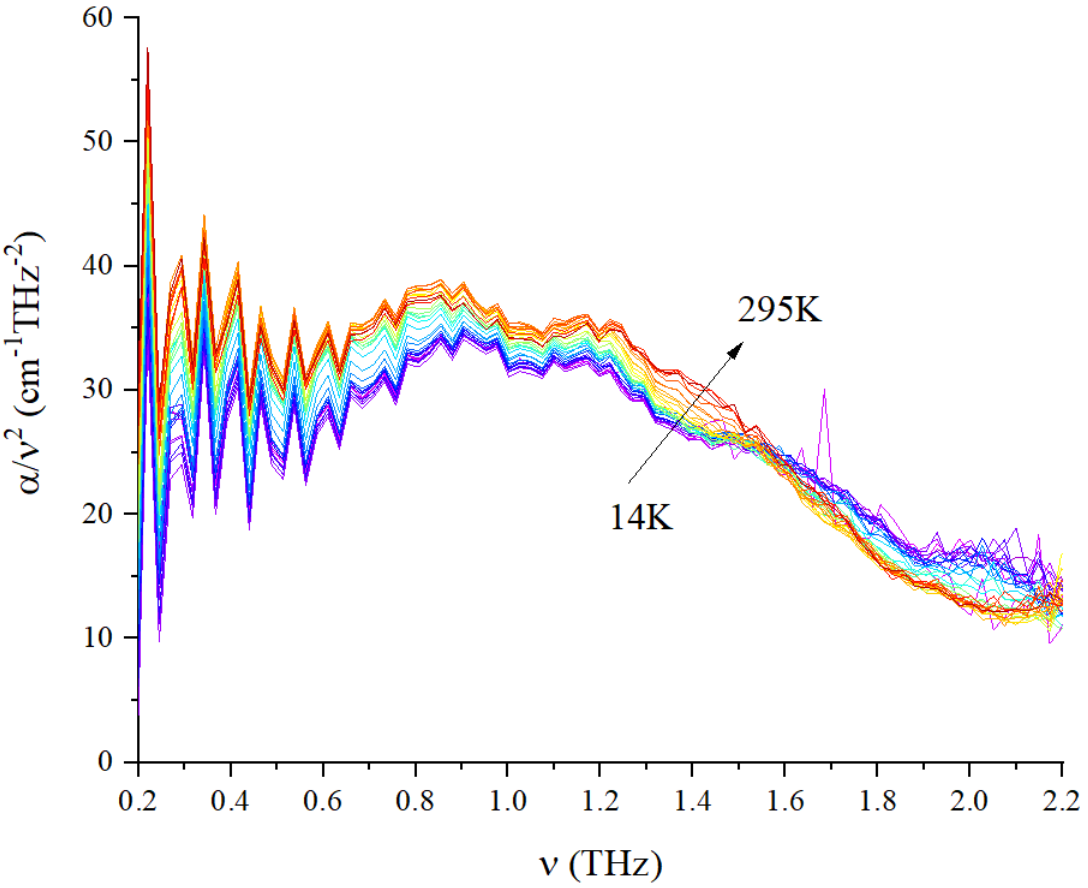

Figure 5.6: Heating THz-TDS measurements of 1.5mm thick 1-FAda sample (in HDP cast) from 14K to 295K as a function of frequency. We can see a clear and broad peak around 1THz, the Boson Peak. For heating rates refer to table 4.2.

results and see whether we appreciate any changes regarding structural conformation, the imaginary part of the complex dielectric permittivity is shown as a function of temperature. The results are displayed on figure 5.7, where we can clearly see the different phase regions and phase transition temperatures.

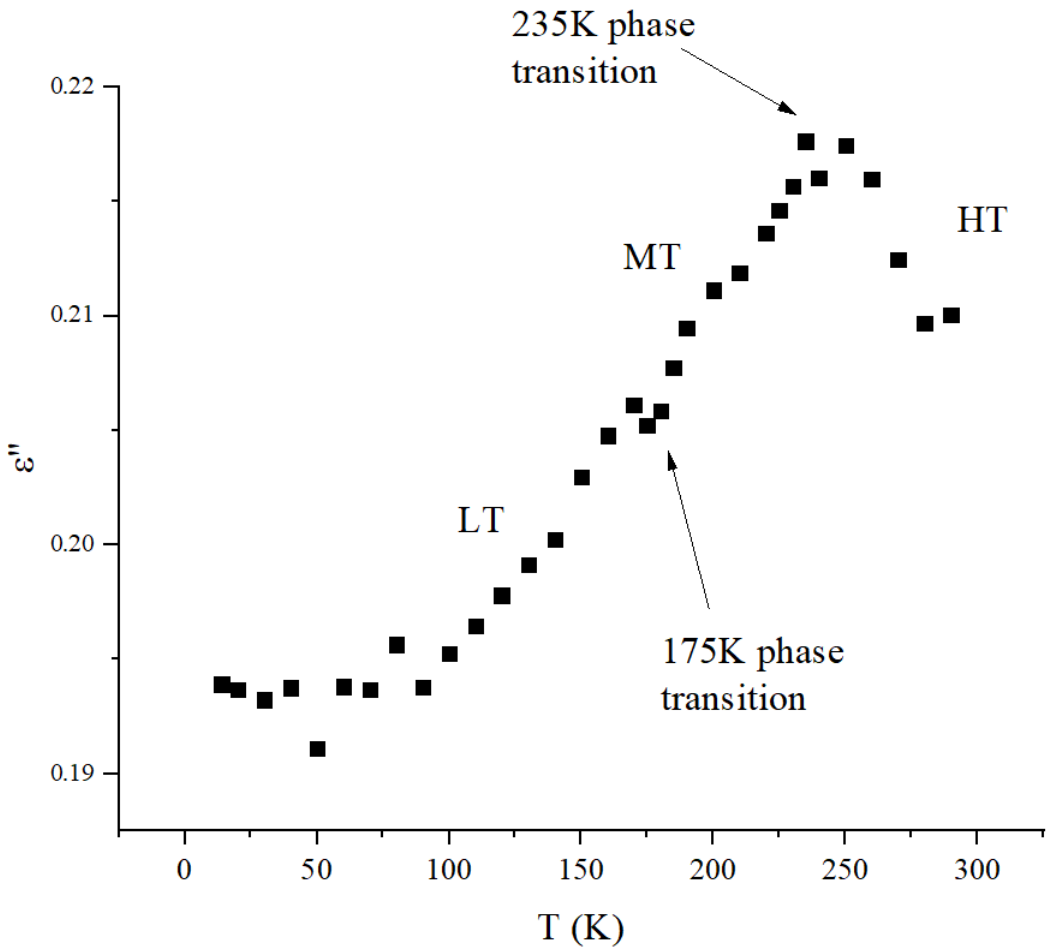

Figure 5.7: Imaginary part of the complex dielectric permittivity vs temperaturefor a 1-FAda heating THz-TDS measurement from 14K up to room temperature at 1THz on a 1.5mm thick sample (with HDP cast). The different phases as well as phase transitions are denoted in the graph.

Chapter 6

Discussion

On a first few notes, we must address the results directly and compare them to the predictions that were made from the previous measurements.

In the case of PCNB, the Boson Peak was successfully identified at 0.5THz, which fits the previous measurements that predicted the appearance around 2meV from inelastic neutron scattering and specific heat results [2]. In that sense PCNB behaved accordingly to the predictions, which highlights the solidness of the previous works as well as the presented results. There are two main points that need to be discussed extensively apart from the Boson Peak appearance: the 1THz peak seen on the α/ν^2 spectra, and the fact that the Boson Peak can only be seen on temperatures lower than 270K.

For 1-FAda, the Boson peak was identified around 1THz, thus behaving accordingly to the previous measurements performed by GCM on inelastic neutron scattering that predicted its position around 4meV.

6.1 PCNB discussion

By means of the results we have seen that for a thick enough sample and a mild cooling we can obtain a clear evidence of the Boson Peak presented by PCNB on a frequency range spanning from 0.48THz to 0.43THz. We see for lower temperatures a higher associated Boson Peak frequency, whilst this frequency shifts very slightly to lower frequencies for higher temperatures. This phenomenon is observed throughout a lot of different THz-TDS measurements and other calculations where the slight displacement of the Boson Peak is assumed to be caused by either a Morse Potential model [44] or/and a change in the diffusivity of the system given the temperature change. We will see these phenomenon in both materials.

According to the Morse Potential model, as seen on figure 6.1, when increasing the temperature (and thus, the energy of the system) our eigenvalues experience a clear shift from the assumed energy levels with respects to the harmonic potential eigenvalues. The assumption of this potential model is held as well by the even clearer shift suffered by the 1THz peak, as its energy level is higher, the shift due to heating is even bigger (1.15THz to 1.02THz), which matches the model.

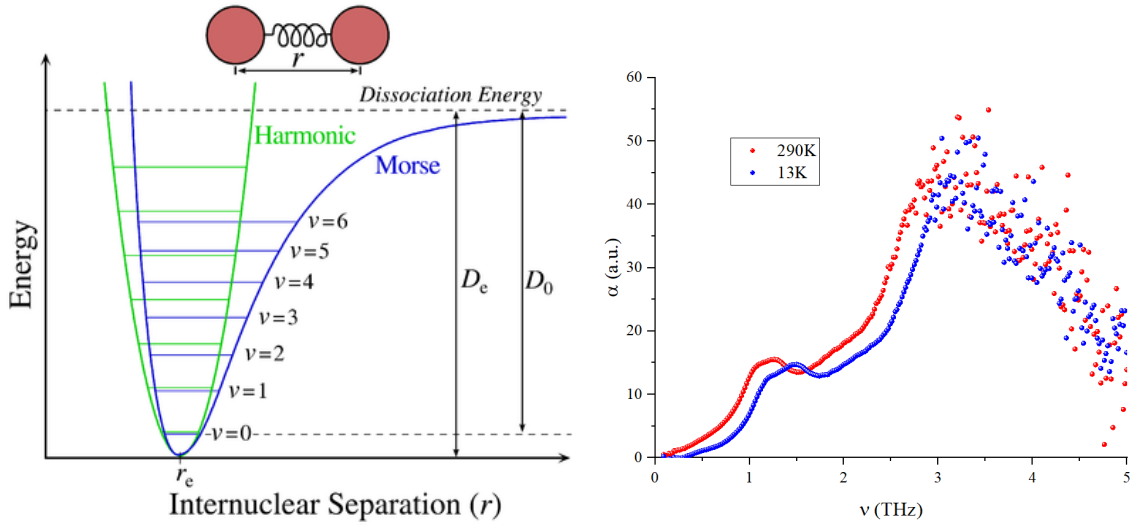

(a) (b)

Figure 6.1: (a) Scheme of the Morse potential (blue curve) versus the harmonic potential (green curve). Instead of having a constant $\hbar\omega$ separation between levels, the Morse potential level spacing decreases as the energy approaches the dissociation energy. (b) Direct comparison of THz-TDS results for a measurement from 13K and 295K run. We see the clear shift of the whole spectra assumed to be caused by diffusivity increase and the Morse potential associated with the system.

On the other hand, according to the previous works performed by *Zaccone et Baggioli* [45], on which taking the assumption that the dynamics of the system are well-described by an associate Green function, a clear shift towards lower temperatures is expected when increasing the diffusivity of the system (in this case, via heating).

Regarding the behaviour of the Boson Peak itself, we see that its profile and broadness is not consistent throughout the whole measurement. If we compare these results with other glassy materials measured by the same laboratory [46][39][34][47][36] we can observe that the broadness is affected by different variables that include the heating. Thus, this broadness must not be a topic of concern when analyzing the data. However, what needs to be addressed is the fact that the Boson peak can't be seen over 270K, and this is believed to be caused by a strong α relaxation that gets activated at higher temperatures and gives us this sudden absorption increase.

With the obtained results, the objective of identifying the Boson Peak on PCNB has been fulfilled. The previous studies performed on the material were predicting such findings, but no result obtained was valid enough to confirm the presence of the Boson Peak on the VDOS of due to the limiting value of the lower energy (around 1.5 meV) at which measurements were done by inelastic neutron scattering.

The questions that now emerge on the topic is the origin of such Boson Peak around 2meV. From the many hypothesis presented on the background chapter, only a few seem to grasp the complexity of this system. The studied material is not con-

sidered an amorphous solid, given its crystalline condition, there is no apparent inversion symmetries on the system, and nevertheless there is a clear appearance of the Boson Peak. It has been seen in other materials such as 2-adamantanone [38] and demonstrated by theoretical studies [11] that the presence of low-lying optical phonons may cause an interaction with the acoustic phonons of similar energies we call hybridization, giving rise to new excess modes that make up the Boson Peak.

In the case of PCNB it has been seen previously that the high energy modes ($\sim 13meV$) we can see on the dielectric spectra correspond to torsion modes of the NO_2 group and librations of the molecule, which are already mainly collective modes associated with low energies. Then, following such line of thought, the modes present on the 1THz peak may very much possibly be collective modes as well. In fact, given the large broadness of the peak and the fact that its broadness does not change when heating (heating should induce a broadening of the modes by themselves), we believe the 1THz peak to be a combination of similar energy collective modes, which can be perfectly identified between $3-6meV$ on the VDOS spectra of PCNB (3.3c). In the cases of studied crystals it is believed for disorder to be a main aspect in the lowering of the energies associated with optic modes [48], and in the case of PCNB it is of no surprise to have low-energy collective optical modes, as it is a material that possesses orientational disorder and whose atomic groups present fairly large displacements from its natural site of lower energy, as shown by *Thomas et al.* [7] and *Cole et al.* [4], which would also contribute to lowering the energies of such optic modes.

Given the previous evidence and the fact that we already see collective modes at 1THz, we believe there is a possible existence of optic phonon dispersion bands around the $2meV$ energy level, which is the energy where the Boson Peak is observed. This gives strength to the hypothesis of optical phonon hybridization in the case regarding PCNB at least. This possibility of a close interaction between optic and acoustic modes has been brought up by a few groups as a way of explaining the emergence of the Boson Peak on an empirically based set of evidence, on which we can always identify the emergence of glassy behaviours on crystals that exhibit low-lying optical phonons on the same energy range as their acoustic phonons. There is also evidence of perfectly ordered phases that continue to exhibit such glassy properties, that would be the forementioned case of 2-Adamantanone, for which its ordered phase was obtained and shown to exhibit the emergence of the Boson Peak on its specific heat, a plateau on its thermal conductivity and presence of optic phonon bands on the corresponding energies. So we can subtract from the necessary requirements to observing the Boson Peak the existence of disorder within our material.

The possibility of the 1THz peak to be a Van Hove singularity was also considered, but then, if we stood by the theory developed by M. Baggioli and A. Zaccone, such shift seen when heating would not be characteristic of a Van Hove singularity. In order to gain a crucial insight on the origin and nature of the Boson Peak, a simulation approach would be necessary in order to visualize the phonon dispersion bands and thus confirm the existence of the presumed $2meV$ optical modes and to discard the option of the 1THz peak being a Van Hove singularity (by analyzing the

bands' gradient, as the Van Hove singularity appears when a band hits null slope).

In addition to the THz-TDS data, a Low-ν Raman Spectroscopy was provided by Ritsumeikan University, which is displayed in figure 6.2. In our case confocal micro-Raman measurements were performed with a depolarised back-scattering geometry. A frequency-doubled diode-pumped solid-state Nd:yttrium-aluminum-garnet laser oscillating in a single longitudinal mode at 532nm (Oxxius LMX-300S) was employed as the excitation source. A homemade microscope with ultranarrow-band notch filters (OptiGrate) was used to focus the excitation laser and collect the Raman-scattered light. The scattered light was analysed using a single monochromator (Jovin-Yvon, HR320, 1200 grooves/mm) equipped with a charge-coupled device camera (Andor, DU420). [49]

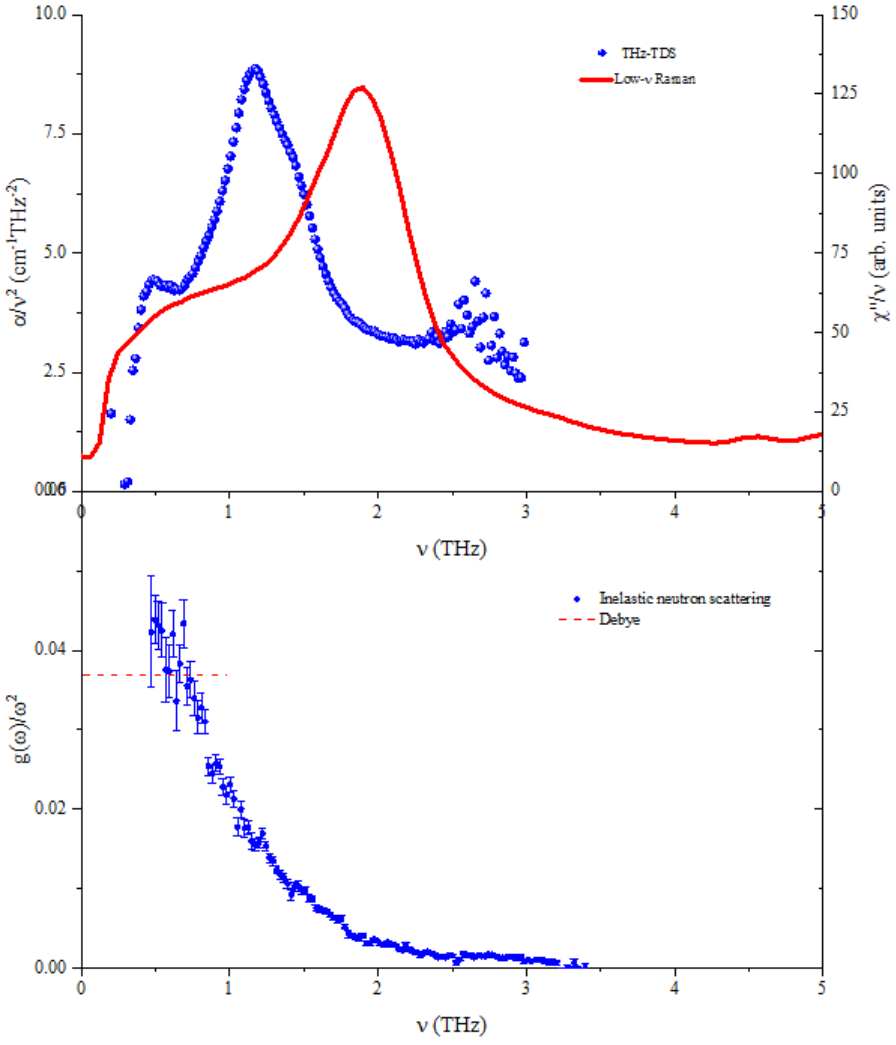

Figure 6.2: Comparison of THz-TDS absorbance divided by frequency squared spectrum of a 4.922mm thick PCNB sample at 13K (blue dots) with Raman susceptibility low-ν Raman scattering measurement of 0.8mm thick PCNB sample at room temperature (red line). VDOS divided by ω^2 obtained from INS measurements is included on the figure below for comparison.

In the case of Raman Susceptibility (χ''), based off different previous works [33] we

know it is capable of detecting the presence of the Boson Peak when divided by the frequency. We see in figure 6.2 that the position of the Boson Peak (approximately 0.5THz) is consistent in both measurements, as for THz-TDS the peak has been located at 0.5THz with heating measurements, and for Raman scattering, the Boson Peak is to be located in the shoulder presented at lower frequencies (around 0.45-0.65THz). Then, with this result we can fairly see the true connection of the Boson Peak with acoustic modes on the lattice, as the position of the Boson Peak remains the same, whilst all the other peaks are displaced because of its optic nature. Of course, such connection further strengthens our hypothesis of hybridization with acoustic modes.

6.2 1-FAda discussion

To begin the discussion of 1-FAda results we would like to address the fact that on the early stages of measurement, when comparing to previous results on other organic materials, the presence of a Boson Peak at 1THz was expected. Let's take the case of glassy glucose [34]: these are both somewhat cyclic organic materials with similar atoms in respect to molecular mass (Oxygen and Fluorine), so we could expect for them to behave similarly, minding the gap between both materials and structures. A clear comparison of both is displayed on figure 6.3. We can see the tendency of glucose as to where we have the emergence of the Boson Peak, and clearly, that was a motivational factor contributing to wanting to cool down 1-FAda and see if the curve profile would behave as expected.

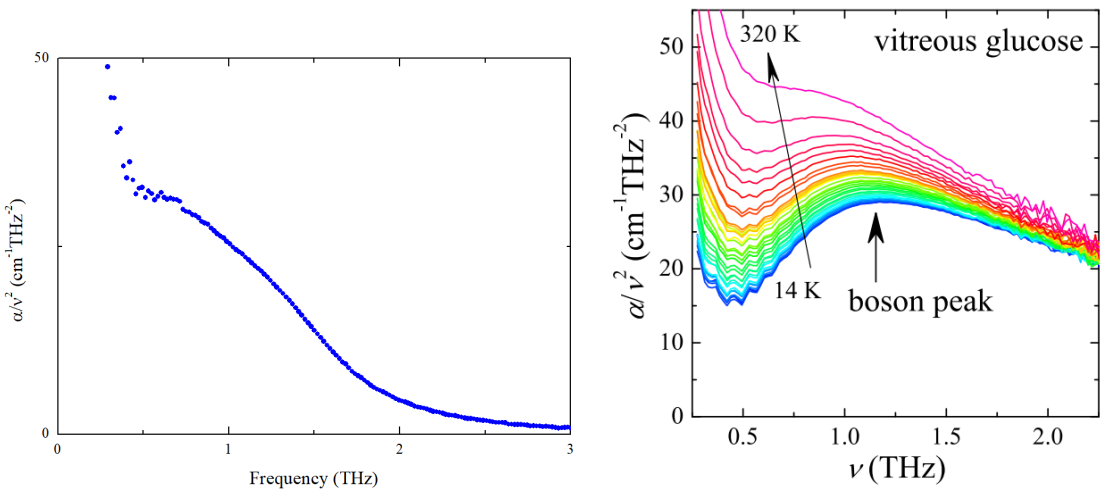

(a) (b)

Figure 6.3: (a) THz-TDS measurement at room temperature of 1-FAda. (b) THz-TDS heating measurement of glassy glucose. We can see the resemblance of the spectra at higher temperatures, so we can assume the trend of glucose to be possibly present in 1-FAda as well.

And so, as seen in the results, such expected behaviour translated into the measurements. The Boson Peak is located at around 1THz and is clearly seen at all temperatures from 14K to 295K. The fact that at room temperature the Boson Peak was initially non-observable is due to a long-term α-relaxation that took place

at those low frequencies, and given the nature of the heating measurement, this relaxation's effect eventually decreased. Knowing that the Boson Peak is present in all temperatures and that it does not seem to show any critical frequency shift throughout, we must take a look at the phase effects on the measurements.

If we now take a look at figure 5.7 from the previous results chapter, the different regions corresponding to the phases of 1-FAda are perfectly defined. These can present different slopes because of the activation of relaxations when heating, which depending on its effect will hinder or enhance the permittivity. No apparent anomalous behaviour is noticed on the regions which correspond to the phase change on the absorbance spectra, thus providing us reasons to believe that the centrosymmetric character of the lattice (which varies from the intermediate temperature phase to low temperature phase) does not affect in any way to the intensity nor position of the Boson Peak. The previously mentioned Nonaffine/inversion-symmetry model then does not fit on the results obtained, as the change in the symmetry of the lattice should give out a response of some sort on the absorbance spectra.

Chapter 7

Conclusions

Both 1-FAda and PCNB THz-TDS measurements have been successfully performed and the output has given a great insight on the dielectric properties of orientationally disordered crystals, as well as universal glassy behaviour.

As far as PCNB is concerned, measurements were compared with previous results and we can be completely sure of the validity of the THZ-TDS measurement, as we could find the glassy temperature at around 185K and the spectrum profile was confirmed with previous far-IR absorption measurements [5]. We have also demonstrated the existence of an α-relaxation, whose presence was detected at high temperatures.

More importantly the Boson Peak was located at 0.45THz, thus validating previous assumptions made by GCM from the INS measurements performed on PCNB. The height of the peak and its broadness become overshadowed by a larger peak at 1THz, but we can fairly say that the Boson Peak frequency is not strongly correlated with temperature (see Annex 1), as most of the profile shift was related to a Morse-potential-associated shift. The 1THz peak is believed to be a group of different intramolecular modes which add up to create this large and broad peak. It is believed that, in fact, it corresponds to a group of modes as the profile and broadness of the peak does not change with temperature, which could only be explained by the peak being formed by different contributions. Finally, the presence of collective modes at very low energies was shown to go with the existence of the 1THz peak, as it is believed by former studies that even the higher frequency modes detected on our results at 2.3THz already belong to collective-like torsion modes. With such proof the hypothesis of interaction between collective optical modes and acoustic modes gains significant strength, but must be confirmed with a clear depiction of the optical and acoustic branches.

As for 1-FAda, we see that the results match perfectly with the previous specific heat measurements that predicted a Boson Peak at 1THz, and we now know that is the exact case for 1-FAda.

More importantly, we see no dependence on the Boson Peak intensity or shape with respect to the different phase changes that 1-FAda displays throughout heating. The lattice centrosymmetricallity does not have any evident effect on collective modes around 1THz, whereas its consequences are clearly seen on higher frequencies. This result not only weakens the Nonaffine/inversion-symmetry model as a universal way of explaining glassy behaviours, but further strengthens the hybridization of low-energy optical phonons theory, as we do expect to find such low-energy collective modes on 1-FAda, like it was done to its closely-related compound 2-Adamantanone.

To sum up, this project has provided further proof of the hybridization hypothesis, as well as a confirmation of previous work performed by the GCM. Additionally, the idea twinning Van Hove singularity and Boson Peak has been discarded from the obtained results. We believe that in order to explain such anomalies on a universal level for disordered solids, the closest depiction at hand has to be the Low-Energy optical phonon hybridization model.

Chapter 8

Further work

In order to fully understand the origin of the Boson Peak there is still a need for the active search of glassy behaviours in atypical disordered materials. The fact that crystals present a Boson Peak on its spectra already defeats the original meaning given to the Boson Peak, so by analyzing different materials with specific properties, it is possible to narrow down the requirements for a material to present a Boson Peak.

In the case of PCNB and 1-FAda it would be interesting to compute the ordered phases of each, as they can be analysed via DFT, but this milestone does not seem at all easy. As for ordered phases, we could take a perfect look at the dispersion branches and determine whether it is the presence of the suspected low-E optical phonons the source of the excess on the VDOS. To date, this has proven to be the most appropriate theory for the particular materials studied by the GCM.

To improve our results and analyses we should perform a Low-ν Raman Scattering for both samples, but specially PCNB, as addressing the origin of the 1THz peak is crucial in order to possibly relating it to the Boson Peak. A Low-ν Raman Scattering measurement was planned during the stay, but given the circumstances no results were obtained till middle of June. We believe that these data would be very helpful in describing the universal behavior of disordered materials such as PCNB and 1-FAda.

Appendix A

Boson Peak frequency as a function of temperature on PCNB

From the data obtained on the THz-TDS measurement on heating of a 4.922mm thick PCNB sample we were able to determine the exact Boson Peak position on each temperature. This position was obtained via fitting of the imaginary part of the complex permittivity on a region span from 0.402THz to 0.586THz, and proceeding to locate the inflexion point of such region.

The results are the following:

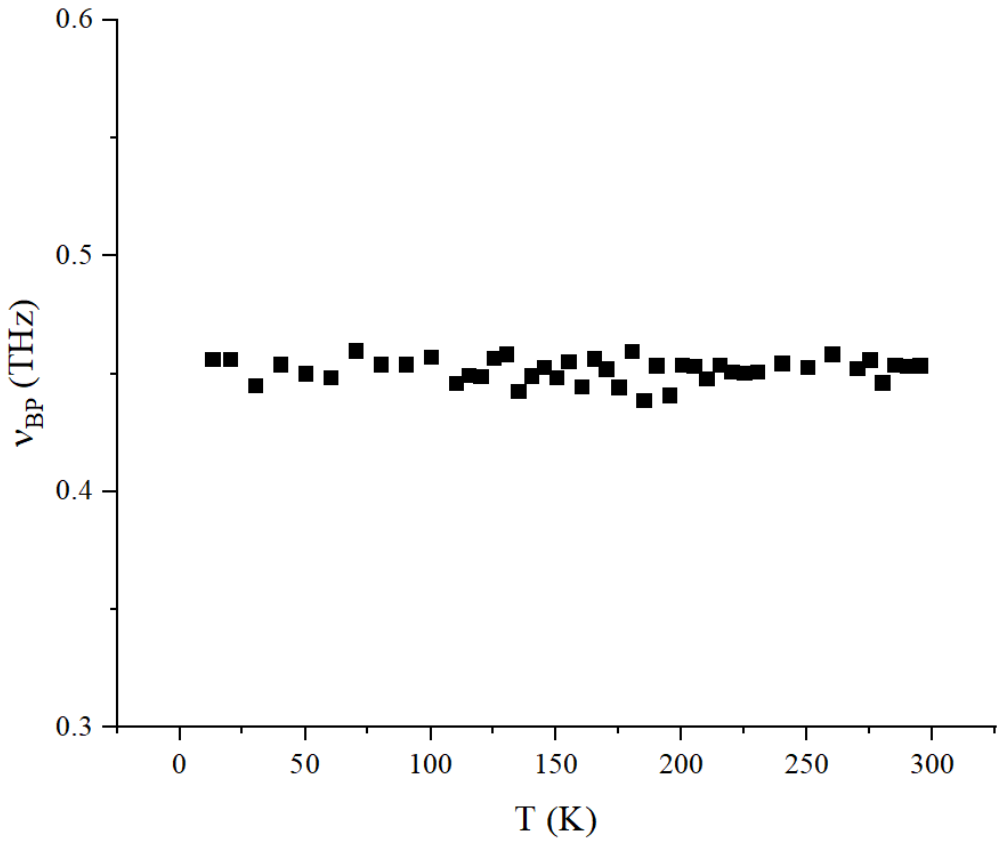

Figure A.1: Boson Peak frequency as a function of temperature on a 4.922mm thick PCNB sample.

Bibliography

[1] S. R. Elliott, *Physics of Amorphous Materials* (Longman, New York, 1990).

[2] J. F. Gebbia, M. A. Ramos, D. Szewczyk, A. Jezowski, A. I. Krivchikov, Y. V. Horbatenko, T. Guidi, F. J. Bermejo, J. Ll. Tamarit, Phys. Rev. Lett. 119(21) (2017).

[3] M. Romanini, M. Barrio, S. Capaccioli, R. Macovez, M. D. Ruiz-Martin, and J. Ll. Tamarit, J. Phys. Chem. C 2016, 120, 19, 10614–10621.

[4] J. M. Cole, H. Burgi, and G. J. McIntyre, Phys. Rev. B 83, 224202 (2011).

[5] C. Reid, G. J. Evans, M. W. Evans, Spectrochimica Acta, Vol.35A pp. 679-680 (1978).

[6] Y. V.Horbatnko, O. O.Romantsova, O. A.Korolyuk, A. Jeżowski, D. Szewczyk, J. Ll. Tamarit, A. I. Krivchikov, J. Phys.Chem.Sol. 127, 151-157 (2019).

[7] L. H. Thomas, T. R. Welberry, D. J. Goossens, A. P. Heerdegen, M. J. Gutmann, S. J. Teat, P. L. Lee, C. C. Wilson and J. M. Cole, Acta Cryst. B63, 663-673 (2007).

[8] L. Yuan, S. Clevers, A. Burel, P. Negrier, M. del Barrio, B. B. Hassine, D. Mondieig, V. Dupray, J. Ll. Tamarit, and G. Coquerel, Cryst. Growth Des. 2017, 17, 6, 3395–3401.

[9] M. A. Ramos, Low Temp. Phys. 46, 104 (2020).

[10] M. Baggioli & A. Zaccone, Phys. Rev. Lett. 122, 145501 (2019).

[11] M. Baggioli & A. Zaccone, J. Phys. Mater. 3, 015004 (2020).

[12] C. Kittel, *Introduction to Solid State Physics, 8th Edition* (Wiley, 2004).

[13] Y. M. Beltukov et al (2013) J. Phys.: Conf. Ser. 461 012044.

[14] Y. M. Beltukov, C. Fusco, D. A. Parshin, and A. Tanguy, Phys. Rev. E 93, 023006 (2016).

[15] For more detailed discussions, see: (a) V. K. Malinovsky, V. N. Novikov, P. P. Parshin, A. P. Sokolov, and M. G. Zemlyanov, *Europhys. Lett.* 11, 43 (1990); M. A. Ramos, *Phys. Rev. B* 49, 702 (1994).

[16] O. A. Korolyuk , A. I. Krivchikov , and O. O. Romantsova, Low Temp. Phys. 46, 111 (2020).

[17] G. A. Vdovichenko, A. I. Krivchikov, O. A. Korolyuk, J. Ll. Tamarit, L. C. Pardo, M. Rovira-Esteva, F. J. Bermejo, M. Hassaine and M. A. Ramos, J. Chem. Phys. 143, 084510 (2015).

[18] Alessio Zaccone, Topical review: *Relaxation and vibrational properties in metal alloys and other disordered systems*. J. Phys. Condes. Matter. 32. 203001. (2020).

[19] Nakayama, Tsuneyoshi (2002). *Boson peak and terahertz frequency dynamics of vitreous silica*. Reports on Progress in Physics, 65(8), 1195-1242.

[20] A. I. Chumakov, G. Monaco, A. Monaco, W. A. Crichton, A. Bosak, R. Rüffer, A. Meyer, F. Kargl, L. Comez, D. Fioretto, H. Giefers, S. Roitsch, G. Wortmann, M. H. Manghnani, A. Hushur, Q. Williams, J. Balogh, K. Parliński, P. Jochym, and P. Piekarz, Phys. Rev. Lett. 106, 225501 (2011).

[21] W. Schirmacher, Europhys. Lett. 73, 6 (2006).

[22] W. Schirmacher, G. Ruocco & T. Scopigno, "Acoustic attenuation in glasses and its relation with the boson peak," Phys. Rev. Lett., 98, 025501, (2007).

[23] J. Plemelj, *Problems in the sense of Riemann and Klein*. New York: Interscience Publishers (1964).

[24] T. Nakayama, and E. Kanashita, EPL, Vol. 84, 6 (2008).

[25] D. A. Parshin, 1993 Phys. Scr. 1993 180.

[26] D. A. Parshin, Phys. Rev. B.; 49(14):9400-9418 (1994).

[27] V. G. Karpov, M. I. Klinger, and F. N. Ignat'ev, Zh. Eksp. Teor. Fiz. 84, 760 (1983); U. Buchenau, Yu.M. Galperin, V. L. Gurevich, D. A. Parshin, M. A. Ramos, and H. R. Schober, Phys. Rev. B 46, 2798 (1992).

[28] D. A. Parshin, Phys. Rev. B. 49, 9400 (1994).

[29] Pablo Esquinazi, *Tunneling Systems in Amorphous and Crystalline Solids* (Springer-Verlag Berlin Heidelberg, 1998).

[30] A. Lemaître & C. Maloney, *Sum rules for the quasistatic and visco-elastic response of disordered solids at zero temperature*. J. Statist. Phys. 123, 415 (2006)

[31] A. Zaccone & E. Scossa-Romano, *Approximate analytical description of the nonaffine response of amorphous solids*. Phys. Rev. B, vol. 83, p. 184205, May 2011.

[32] S. Alexander, R. Orbach. *Density of states on fractals: " fractons "*. J. Phys. Lett. (Paris), 43(17), 625-631 (1982).

[33] T. Mori, Y. Jiang, Y. Fujii, S. Kitani, H. Mizuno, A. Koreeda, L. Motoji, H. Tokoro, K. Shiraki, Y. Yamamoto, S. Kojima. *Detection of boson peak and fractal dynamics of disordered system using terahertz spectroscopy*, arXiv:1910.04400. (2019).

[34] Z. Junlan, T. Mori, Y. Fujii, T. Kashiwagi, W. Terao, M. Yamashiro, H. Minami, M. Tsujimoto, T. Tanaka, H. Kawashima, J. Ito, M. Kijima, M. Iji, M. Watanabe, K. Kadowaki. *Molecular Vibration and Boson Peak Analysis of Glucose Polymers and Ester via Terahertz Spectroscopy.* Carbohydrate Polymers. 232. 115789. (2019).

[35] S. N. Taraskin, S. I. Simdyankin, S. R. Elliott, J. R. Neilson, and T. Lo, Phys. Rev. Lett. 97, 055504 (2006).

[36] T. Mori et al., *Terahertz Spectroscopy on Myoglobin: Boson Peak and Fracton* 2019 44th International Conference on Infrared, Millimeter, and Terahertz Waves (IRMMW-THz), Paris, France, 2019, pp. 1-2.

[37] S. Taraskin & S. Simdyankin, & S. Elliott, *The atomic charge distribution in glasses obtained by terahertz spectroscopy.* J. Phys. Condens. Matter. 19. 455216. (2007).

[38] D. Szewczyk, A. Jeżowski, G. A Vdovichenko, A. I. Krivchikov, F. J. Bermejo, J. Ll. Tamarit, L. C. Pardo, and J. W. Taylor, J. Phys. Chem. B 2015, 119, 26, 8468–8474.

[39] T. Shibata, T. Mori, S. Kojima *Low-frequency vibrational properties of crystalline and glassy indomethacin probed by terahertz time-domain spectroscopy and low-frequency Raman scattering.* Spectrochim Acta A Mol Biomol Spectrosc. 150, 207-211 (2015).

[40] L. Zhang, J. Zheng, Y. Wang et al. *Experimental studies of vibrational modes in a two-dimensional amorphous solid.* Nat Commun 8, 67 (2017).

[41] A. A. Maradudin & R. F. Wallis, Phys. Rev. 123, 777 (1961).

[42] Taraskin, S.. *Infrared absorption in glasses and their crystalline counterparts.* J. Phys. Condens. Matter. 19. 415113. (2007).

[43] Y. Guinet , J.L. Sauvajol & M. Muller Raman studies of orientational disorder in crystals, Mol. Phys., 65:3, 723-738 (1988).

[44] P. M. Morse, *Diatomic molecules according to the wave mechanics. II. Vibrational levels.* Phys. Rev. 34, 57-64 (1929).

[45] Baggioli, Matteo & Zaccone, Alessio. (2020). *Unified theory of vibrational spectra in hard amorphous materials.* Physical Review Research. 2. 013267.

[46] N. Tomoshige, H. Mizuno, T. Mori et al. *Boson peak, elasticity, and glass transition temperature in polymer glasses: Effects of the rigidity of chain bending.* Sci Rep 9, 19514 (2019).

[47] M. Kabeya, T. Mori, Y. Fujii, A. Koreeda, B. W. Lee, J.H. Ko, and S. Kojima, Phys. Rev. B 94, 224204 (2016).

[48] A. Krivchikov, G.A. Vdovichenko, O.A. Korolyuk, F. Bermejo, L.C. Pardo, J. Ll. Tamarit, A. Jezowski, D. Szewczyk. *Effects of site-occupation disorder on the low-temperature thermal conductivity of molecular crystals.* J. Non-Cryst. Solids 407, 141-148 (2015).

[49] Y. Fujii, D. Katayama & A. Koreeda, *Broadband light scattering spectroscopy utilizing an 20 ultra-narrowband holographic notch filter.* Jpn. J. Appl. Phys. 55 (2016).

[50] M. Dressel and G. Gruner, *Electrodynamics of Solids* (Cambridge University Press, 2002).

[51] M. Moratalla, J. F. Gebbia, M. A. Ramos, L. C. Pardo, S. Mukhopadhyay, S. Rudic, F. Fernandez-Alonso, F. J. Bermejo, and J. Ll. Tamarit, Phys. Rev. B 99, 024301 (2019).

[52] J. S. Tse, V. P. Shpakov, V. V. Murashov, and V. R. Belosludov, J. Chem. Phys. 107, 9271 (1997).

[53] J. S. Tse, V. P. Shpakov, V. R. Belosludov, F. Trouw, Y. P. Handa and W. Press, 2001 Europhys. Lett. 54 354.

[54] M. Simoncelli, N. Marzari & F. Mauri, *Unified theory of thermal transport in crystals and glasses*, Nature Phys. 15, 809–813 (2019).

[55] A. Zaccone, M. Baggioli, C. Setty. *Effective Theory of Superconductivity in Strongly-Coupled Amorphous Materials* (2020).

[56] B. Ben Hassine, Ph. Negrier, M. Romanini, M. Barrio, R. Macovez, A. Kallel, D. Mondieiga and J.Ll. Tamarit, Phys. Chem. Chem. Phys., 18, 10924-10930. (2016).

[57] M.I. Klinger & A.M. Kosevich, *Soft-mode-dynamics model of acoustic-like high-frequency excitations in boson-peak spectra of glasses.* Physics Letters A. 280. 365-370. (2001).

[58] R. L. González-Romero, A. Antonelli, A. S. Chaves and J. J. Meléndez, Phys. Chem. Chem. Phys., 20, 1809-1816 (2018).

[59] A. A. Maradudin and R. F. Wallis, Phys. Rev. 123, 777 (1961).

[60] Y. M. Beltukov, V. I. Kozub, and D. A. Parshin, Phys. Rev. B 87, 134203 (2013).

[61] B. Rufflé, G. Guimbretière, E. Courtens, R. Vacher, and G. Monaco, Phys. Rev. Lett. 96, 045502 (2006).

[62] M. Baggioli and A. Zaccone, Phys. Rev. Lett. 122, 145501 (2019).

[63] U. Buchenau, M. Prager, N. Nücker, A.J. Dianoux, N. Ahmad, W.A. Phillips, Phys. Rev. B 15, 5665-5673 (1986).

[64] H. Shintani, H. Tanaka, *Universal link between the boson peak and transverse phonons in glass.* Nature Mater 7, 870–877 (2008).

[65] M. Kabeya et al. *Boson peak dynamics of glassy glucose studied by integrated terahertz band spectroscopy.* Phys. Rev. B 94, 224204 (2016).